Inorg. Chem. **2008**, *47*, 11570−11582

Group VIII Coordination Chemistry of a Pincer-Type Bis(8-quinolinyl)amido Ligand

Theodore A. Betley,[†] Baixin A. Qian, and Jonas C. Peters*[,‡]

Division of Chemistry and Chemical Engineering, Arnold and Mabel Beckman Laboratories of Chemical Synthesis, California Institute of Technology, Pasadena, California 91125, and Department of Chemistry, Massachusetts Institute of Technology, Cambridge, Massachusetts 02139

Received June 11, 2008

This paper provides an entry point to the coordination chemistry of the group VIII chemistry of the bis(8-quinolinyl)amine (BQA) ligand. In this context, mono- and disubstituted BQA complexes of iron, ruthenium, and osmium are described. For example, the low-spin bis-ligated Fe(III) complex $[Fe(BQA)_2][BPh_4]$ has been prepared via amine addition to $FeCl_3$ in the presence of a base and $NaBPh_4$. Complexes featuring a single BQA ligand are more readily prepared for Ru and Os. Auxiliary ligands featuring a single BQA ligand, along with two other L-type donor ligands, allow for a variety of ligand types to occupy a sixth coordination site. Representative examples include the halide and pseudohalide complexes *trans*-$(BQA)MX(PPh_3)_2$ (M = Ru, Os; X = Cl, Br, N_3, OTf), as well as the hydride and alkyl complexes *trans*-$(BQA)RuH(PMe_3)_2$ and *trans*-$(BQA)RuMe(PMe_3)_2$. Electrochemical studies are discussed that help to contextualize the BQA ligand with respect to its neutral counterpart 2,2′,2″-terpyridine (terpy) in terms of electron-releasing character. Bidentate ligands have been explored in conjunction with the BQA ligand. Thus, the bidentate, monoanionic aryl(8-quinolinyl)amido ligand 3,5-$(CF_3)_2$-(C_6H_3)QA has been installed onto the (BQA)Ru platform to provide $(BQA)Ru(3,5\text{-}(CF_3)_2\text{-}(C_6H_3)QA)(PPh_3)$. A bis(phosphino)borate ligand stabilizes the five-coordinate complex $[Ph_2B(CH_2PPh_2)_2]Ru(BQA)$. Finally, access to dinitrogen complexes of the types $[(BQA)Ru(N_2)(PPh_3)_2][PF_6]$, $[(BQA)Ru(N_2)(PMe_3)_2][PF_6]$, and $[(BQA)Os(N_2)(PPh_3)_2][PF_6]$ is provided by exposure of the sixth coordination site under a N_2 atmosphere.

Introduction

Some years ago, the term "pincer-type amido" ligand was introduced to refer to anionic tridentate ligands that feature a central X-type metal−amido linkage with two chelating donor arms extending from this central donor.[1] The use of the term "pincer" implied amido ligands that would most commonly favor a planar binding geometry such that, when coordinated to an octahedral metal complex, they would display a mer binding configuration. In this regard, such ligands are conceptually analogous to the more popular family of anionic "pincer" ligands in which a central carbon rather than nitrogen X-type linkage binds the metal. A prototypical example of the latter ligand type is a cyclometalated arylbis(phosphine), and related systems where the donors are amines, carbenes, and other donors are also well established.[2−4]

In the past several years, "pincer-type" amido ligands have gained prominence in organometallic and inorganic chemistry,[5,6] the most popular examples of such systems being diarylamido ligands in which two phosphine donors extend

* Author to whom correspondence should be addressed. E-mail: jcpeters@mit.edu.
† Current address: Harvard University, Cambridge MA.
‡ Current address: Massachusetts Institute of Technology, 77 Massachusetts Ave Cambridge, MA 02139.

(1) Peters, J. C.; Harkins, S. B.; Brown, S. D. *Inorg. Chem.* **2001**, *40*, 5083.
(2) (a) Pugh, D.; Danopoulos, A. A. *Coord. Chem. Rev.* **2007**, *251*, 610. (b) van der Boom, M. E.; Milstein, D. *Chem. Rev.* **2003**, *103*, 1759. (c) Gossage, R. A.; Van De Kuil, L. A.; van Koten, G. *Acc. Chem. Res.* **1998**, *31*, 423.
(3) (a) Liu, F. C.; Pak, E. B.; Singh, B.; Jensen, C. M.; Goldman, A. S. *J. Am. Chem. Soc.* **1999**, *121*, 4086. (b) Sundermann, A.; Uzan, O.; Milstein, D.; Martin, J. M. L. *J. Am. Chem. Soc.* **2000**, *122*, 7095. (c) Dani, P.; Karlen, T.; Gossage, R. A.; Gladiali, S.; van Koten, G. *Angew. Chem., Int. Ed.* **2000**, *39*, 743.
(4) (a) Mayer, H. A.; Kaska, W. C. *Chem. Rev.* **1994**, *94*, 1239. (b) Bianchini, C.; Meli, A.; Peruzzini, M.; Vizza, F.; Zanobini, F. *Coord. Chem. Rev.* **1992**, *120*, 193. (c) Cotton, F. A.; Hong, B. *Prog. Inorg. Chem.* **1992**, *40*, 179.
(5) Liang, L. C.; Lin, J. M.; Hung, C. H. *Organometallics* **2003**, *22*, 3007.
(6) Harkins, S. B.; Peters, J. C. *J. Am. Chem. Soc.* **2004**, *126*, 2885.

10.1021/ic801047s CCC: $40.75
Published on Web 11/13/2008

Scheme 1

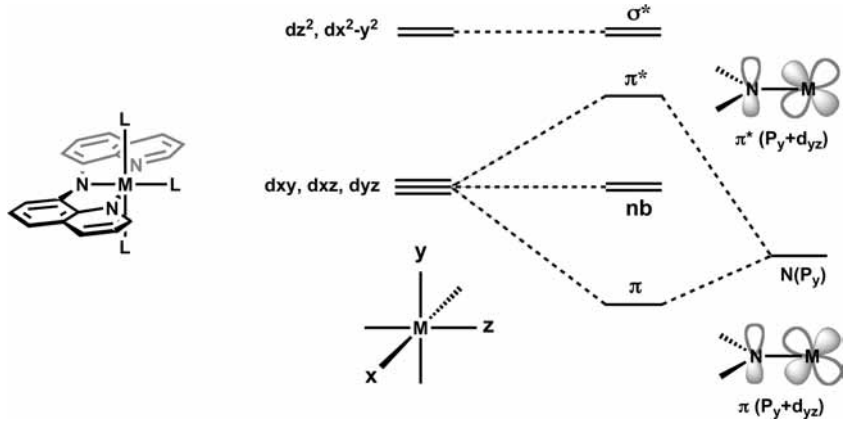

from the ortho positions of the aryl rings.[7] These ligands closely resemble the hard/soft bis(phosphine)amido ligands that were originally introduced by Fryzuk.[8] Indeed, while it is often assumed that the diarylamido bis(donor) ligands will adopt a rigid planar geometry owing to the aryl bridging units, such ligands are in fact conformationally quite flexible and, like the earlier Fryzuk systems, give rise to more diverse structure types. [9]

The pincer-type bis(8-quinolinyl)amido ligand, which presents two sp^2-hybridized hard N donors to a chelated metal ion in addition to the diarylamido unit, is perhaps more highly disposed to bind in a planar fashion; it was hence for this ligand system that the term "pincer-type" amido ligand was first coined.[1] However, even this ligand can adopt a facial binding motif, as shown for an octahedral Pt(IV) system.[9c] Nevertheless, we and others have generally found that this ligand is most typically disposed to a planar binding motif[1,9c,10,11] and is, moreover, a robust chelate even in the presence of aqueous and acidic solvents. These properties distinguish it from many other amido ligands, whether or not they are stabilized by a chelate effect, for which aminolysis can be both kinetically and thermodynamically problematic. In this regard, bis(8-quinolinyl)amido ligands have many properties in common with conjugated aromatic N-heterocyclic chelates, such as the ubiquitous 2,2′,2″-terpyridine (terpy) ligand,[12] and should likewise be robust under relatively oxidizing conditions owing to the exclusive presence of hard N donors conjugated into an aromatic π system. However, as the bis(8-quinolinyl)amine (BQA) ligand is typically monoanionic when coordinated to a metal, rather than a neutral donor as for terpy, its resulting metal complexes should be appreciably more electron-rich than terpy relatives, a property that is potentially advantageous for reductive small molecule activation reactions.

To begin to more thoroughly explore the advantages and disadvantages of the bis(8-quinolinyl)amido auxiliary as a conveniently synthesized, monanionic "pincer" analogue of terpyridine, we have undertaken the preparation and study of a series of group VIII coordination complexes supported by BQA. These systems are cousins of tridentate and planar 2,6-bis(phosphino)aryl-Ru(II) (i.e., PCP-Ru(II)) complexes that have been studied in recent years,[13] for example, in the context of transfer dehydrogenation reactions.[14] However, in octahedral d^6 complexes of the type described herein, a filled amido N(2p) orbital is of appropriate symmetry to mix with a filled metal d orbital (see Scheme 1). If significant mixing occurs, the highest occupied molecular orbital (HOMO) is raised in energy. This HOMO-raising can in principle manifest itself at the metal complex by an increased affinity for π-acidic ligands, or conversely, by a decreased affinity for π-basic ligands.

Results and Discussion

Preparation of $[Fe(BQA)_2][BPh_4]$. To obtain electrochemical data of $M(BQA)_2$ species for comparison with ferrocene, we sought to prepare $Fe(BQA)_2$. We have previously found that delivery of the bis(quinolinyl)amine (HBQA, **1**) ligand to group 10 metals could be achieved via two routes: reaction of a metal halide with **1**[Li] or reaction of the free amine **1** with a metal precursor in the presence of excess base.[1] Metalation of the BQA ligand was carried out with $FeCl_3$ (anhydrous) via an in situ salt metathesis reaction (eq 1). Reacting two equivalents of amine **1** with $FeCl_3$ in dichloromethane with the addition of Na_2CO_3 in water results in rapid formation of the desired complex $[Fe(BQA)_2][Cl]$. The addition of an aqueous solution of

(7) Liang, L. C. *Coord. Chem. Rev.* **2006**, *250*, 1152.
(8) Fryzuk, M. D. *Can. J. Chem.* **1992**, *70*, 2839.
(9) (a) Harkins, S. B.; Peters, J. C. *J. Am. Chem. Soc.* **2004**, *126*, 2885. (b) Harkins, S. B.; Peters, J. C. *J. Am. Chem. Soc.* **2005**, *127*, 2030. (c) Harkins, S. B.; Peters, J. C. *Inorg. Chem.* **2006**, *45*, 4316. (d) Fout, A. R.; Basuli, F.; Fan, H. J.; Tomaszewski, J.; Huffman, J. C.; Baik, M. H.; Mindiola, D. J. *Angew. Chem., Int. Ed.* **2006**, *45*, 3291.
(10) (a) Jenson, K. A.; Nielson, P. H. *Acta Chem. Scand.* **1964**, *18*, 1. (b) Puzas, J. P.; Nakon, R.; Pertersen, J. L. *Inorg. Chem.* **1986**, *25*, 3837.
(11) Maiti, D.; Paul, H.; Chanda, N.; Chakraborty, S.; Mondal, B.; Puranik, V. G.; Lahiri, G. K. *Polyhedron* **2004**, 831.
(12) Sauvage, J.-P.; Collin, J.-P.; Chambron, J.-C.; Guillerez, S.; Coudret, C.; Balzani, V.; Barigelletti, F.; De Cola, L.; Flamigni, L. *Chem. Rev.* **1994**, *94*, 993.
(13) (a) Gusev, D. G.; Madott, M.; Dolgushin, F. M.; Lyssenko, K. A.; Antipin, M. Y *Organometallics* **2000**, *19*, 1734. (b) Regis, R. M.; Rozenberg, H.; Shimon, L. J. W.; Milstein, D. *Organometallics* **2001**, *20*, 1719. (c) Dani, P.; Karlen, T.; Gossage, R. A.; Smeets, W. J. J.; Spek, A. L.; van Koten, G. *J. Am. Chem. Soc.* **1997**, *119*, 11317. (d) Jia, G.; Lee, H. M.; Xia, H. P.; Williams, I. D. *Organometallics* **1996**, *15*, 5453.
(14) Dani, P.; Karlen, T.; Gossage, R. A.; Gladiali, S.; van Koten, G. *Angew. Chem., Int. Ed.* **2000**, *39*, 743.

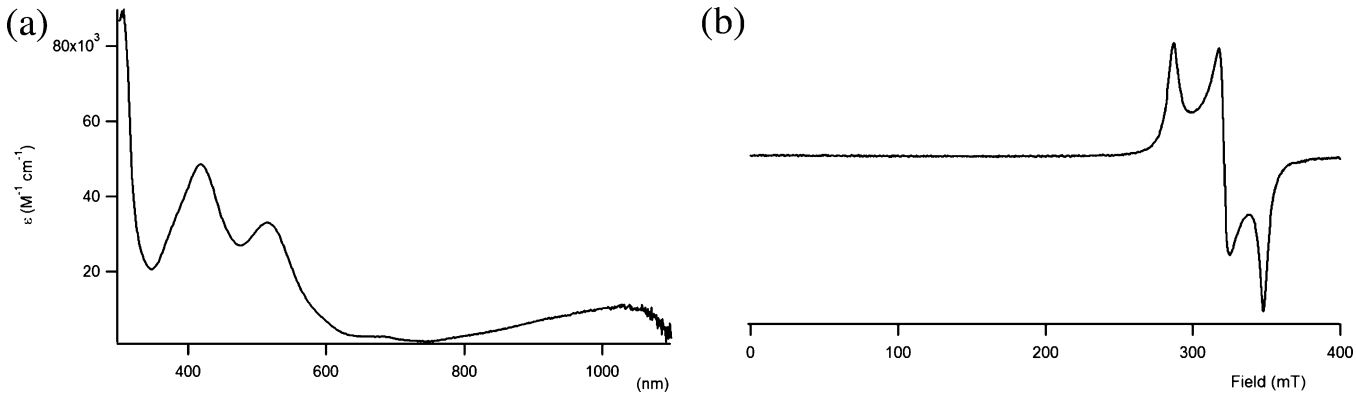

Figure 1. (a) Electronic spectrum of $[Fe(BQA)_2][BPh_4]$ (**2**). (b) EPR spectrum of solid **2** (4 K, X-band, 9.62 GHz).

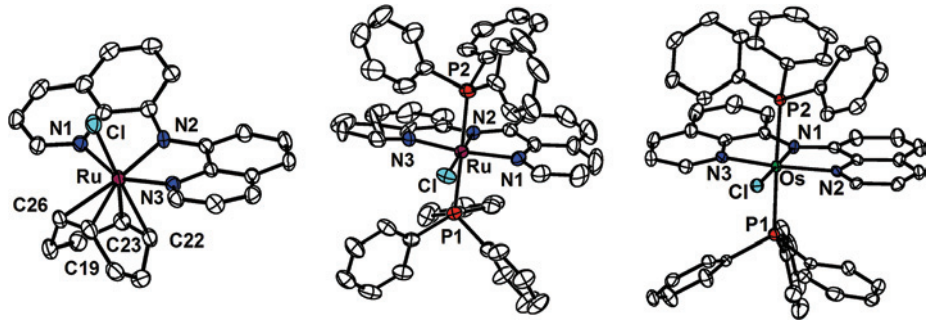

Figure 2. Displacement ellipsoid representation (50%) of (a) (BQA)RuCl(cod) (**3**), (b) (BQA)RuCl$(PPh_3)_2$ (**5**), and (c) (BQA)OsCl$(PPh_3)_2$ (**6**). Hydrogen atoms have been removed for clarity. Selected bond distances (Å) and angles (deg) for **3**: Ru−N1 2.128(3), Ru−N2 2.048(2), Ru−N3 2.126(3), Ru−Cl 2.426(1), avg. Ru−C 2.215(3), N1−Ru−N2 76.9(1), N2−Ru−N3 77.9(1), N1−Ru−N3 151.5(1). For **5**: Ru−N1 2.066(3), Ru−N2 2.005(2), Ru−N3 2.061(3), Ru−Cl 2.482(1), Ru−P1 2.397(1), Ru−P2 2.379(1), N1−Ru−N2 80.4(1), N2−Ru−N3 80.3(1), N1−Ru−N3 160.7(1), P1−Ru−P2 178.9(1). For **6**: Os−N1 2.063(3), Os−N2 2.023(3), Os−N3 2.064(3), Os−Cl 2.488(1), Os−P1 2.368(1), Os−P2 2.381(1), N1−Os−N2 81.5(1), N2−Os−N3 80.1(1), N1−Os−N3 161.5(1), P1−Os−P2 174.8(1).

$NaBPh_4$ to the reaction affords $[Fe(BQA)_2][BPh_4]$ (**2**). The resulting brick red, cationic Fe^{III} species is air-stable and is readily soluble in polar solvents (CH_2Cl_2, DMSO). This is distinct from its poorly soluble iron(II) counterpart, $Fe(BQA)_2$, which can be readily generated from $FeCl_2$, HBQA, and NEt_3 (or from **1**[Li] and $FeCl_2$) and identified by electrospray ionization mass spectrometry, but is difficult to isolate in pure form owing to its poor solubility. Complex **2** exhibits paramagnetically shifted ^1H NMR resonances and appears to populate a doublet ground state exclusively ($\mu_{eff} = 2.1\ \mu_B$), as determined by a room-temperature-solution Evans method determination.[15] Iron(III) $\{Fe(terpy)_2\}^{+}$ species are likewise low-spin in nature.[16]

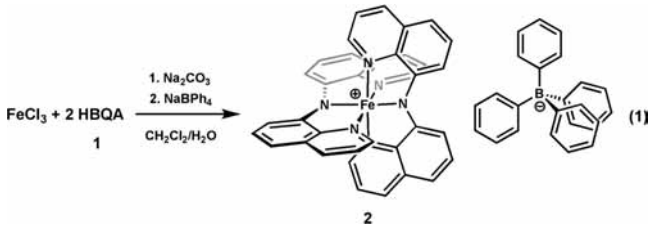

A dichloromethane solution of **2** exhibits multiple intense transitions in the UV−visible region, [λ_{max}/nm (ε/M^{-1} cm^{-1})]: 1030 (11 000), 680 (2700), 514 (33 000), 418 (49 000), 306 (90 000) (Figure 1a). The high extinction coefficients for the intense transitions at 514, 418, and 306 nm are most likely ligand-centered $\pi-\pi^*$ transitions, which is in agreement with the recently assigned spectrum for $[Co(BQA)_2][ClO_4]$ by Lahiri et al.[11] The presence of a weak transition at 680 nm may be the d−d transition ($^3A_1 \rightarrow {}^2T_g$) expected for the d^5 system. The large extinction coefficient for the band at 1030 nm suggests it is a charge-transfer band, quite possibly a ligand-to-metal charge transfer event in which a ligand-centered electron is excited into the singly occupied d orbital.

The EPR of a solid sample of **2** was also collected at 4 K and is shown in Figure 1b. The spin $S = 1/2$ state of **2** gives rise to a rhombic signal where the three **g** tensors are resolved: $g_z = 2.39$, $g_y = 2.14$, $g_x = 1.98$. No hyperfine coupling to nitrogen is observed.

Preparation of Ru and Os BQA Complexes. A single BQA ligand can be installed onto divalent Ru or Os centers from a variety of precursors. For example, the reaction of polymeric $[RuCl_2(COD)]_n$ with one equivalent of **1**[Li] yields (BQA)RuCl(COD) (**3**) and variable amounts (20−30%) of the disubstituted species $Ru(BQA)_2$ (COD = cyclooctadiene). Flash chromatography effectively separates the products. Complex **3** has been characterized in the solid state by X-ray crystallography, and its solid-state structure is shown in Figure 2. Quantitative conversion to the disubstituted species $Ru(BQA)_2$ (**4**) can be achieved by refluxing $[RuCl_2(COD)]_n$ with two equivalents of **1**[Li] in toluene. An electrospray mass spectrum (ES-MS) of the product mixture reveals only the parent ion peak for the disubstituted species, **4**, at $m/z =$

(15) (a) Sur, S. K. *J. Magn. Reson.* **1989**, *82*, 169. (b) Evans, D. F. *J. Chem. Soc.* **1959**, 2003.
(16) Reiff, W. M. *J. Am. Chem. Soc.* **1974**, *96*, 3829.

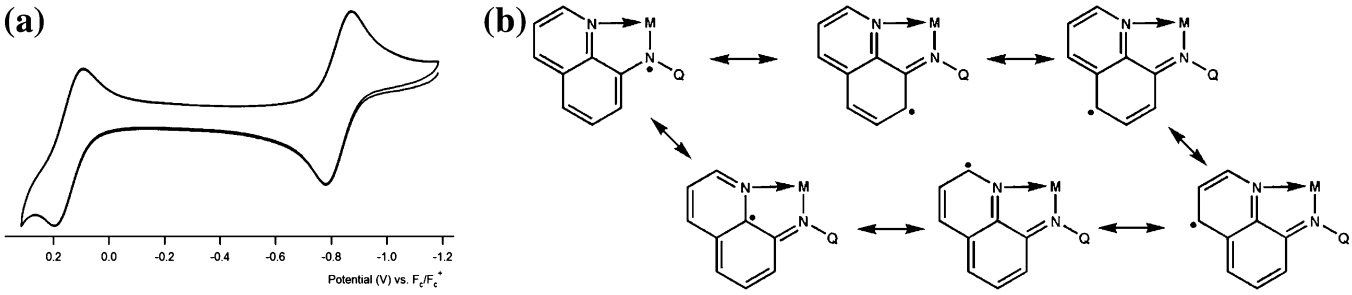

Figure 3. (a) Cyclic voltammetry of **2** in 0.4 M ^{n}Bu$_4$NPF$_6$/THF, scan rate = 75 mV/s. (b) Postulated radical delocalization of the bis(quinolinyl)amide ligand (Q = quinoline).

642, without **3** or any ligand fragmentation products apparent in the spectrum.

Refluxing $RuCl_2(PPh_3)_3$ in dichloromethane with HBQA in the presence of excess base (NEt_3) results in the formation of (BQA)$RuCl(PPh_3)_2$ (**5**), which can be isolated in crystalline yields exceeding 85%. The ^{31}P NMR spectrum of **5** shows a single chemical shift at $\delta = 29$ ppm in benzene, suggesting that the phosphorus nuclei are trans-disposed with the BQA ligand bound in the expected mer fashion. This is confirmed by X-ray diffraction (XRD) analysis (vide infra). Product **5** can also be obtained via salt elimination by the reaction of **1**[Li] and $RuCl_2(PPh_3)_3$ in toluene at room temperature. Similarly, the Os congener (BQA)$OsCl(PPh_3)_2$ (**6**) is produced via the reaction of **1**[Li] and $OsCl_2(PPh_3)_3$ in toluene at room temperature. However, when $OsCl_2(PPh_3)_3$ is exposed to the free amine **1**, in the presence of excess triethylamine base, the product *cis*-$(PPh_3)_2$OsCl(BQA) (**7**) is instead exclusively obtained, as revealed by its ^{31}P NMR spectrum (δ 2.2, -0.9, $^2J_{P-P} = 10.7$ Hz). While **7** can be isolated as a brown solid, all attempts to crystallize it from solution invariably yielded crystals of the green, trans-disposed product **6**, suggesting the latter to be thermally favored on steric grounds. The solid-state crystal structures for complexes **5** and **6** are shown in Figure 2. The solid-state structures for **3**, **5**, and **6** all demonstrate that the BQA ligand binds in a mer fashion. The amido N−M bond distances are consistently shorter ($\Delta \sim 0.06$ Å) than the quinolinyl N−M bond distances. The proclivity for the BQA ligand to "pinch" back is also apparent by the N1−M−N3 bond angles, which range from 150 to 160°. Finally, the BQA ligands display a gentle twist that presumably relieves a steric interaction between the H atoms connected to the C7 positions of the two quinoline arms.

Electrochemical Analysis of (BQA)$_n$M Complexes. It is interesting to compare the $Fe^{III/II}$ redox potentials of **2** to other examples of homoleptic Fe complexes. Figure 3 shows the cyclic voltammogram of **2** in 0.1 M ^{n}Bu$_4$NPF$_6$ in dichloromethane referenced against an internal Fc/Fc$^+$ standard. The $Fe^{III/II}$ couple for **2** ($E_{1/2} = -0.79$ V, $\Delta_p = 65$ mV) is 0.79 V more reducing than the $Fe^{III/II}$ couple for Fc, suggesting that **2** could be used as a mild oxidizing agent.[17] The electron-rich Fe(BQA)$_2$ system features an $Fe^{III/II}$ couple that is at a potential even lower than Cp*$_2$Fe, which exhibits an $Fe^{III/II}$ couple at -0.48 V.[17] In addition to the $Fe^{III/II}$ couple, complex **2** exhibits a second, irreversible redox event at $E_{1/2} = +0.14$ V. The shape of the secondary oxidation event was independent of scan rate (0.05−0.5 V/s) and did not change noticeably when THF or dichloromethane was the solvent. This second redox event could signify a $Fe^{IV/III}$ redox event, or it could represent some redox process centered on the BQA ligand itself. The BQA ligand, which exhibits an irreversible oxidation event at +0.56 V (vs Fc/Fc$^+$), is the most likely the candidate for oxidation in this case. If this second redox event is ligand-centered, the radical thus formed can be delocalized over the quinoline rings of BQA. Possible contributing resonance structures that would serve to stabilize the radical are presented in Figure 3b. In any event, the increase in current that is observed positive in this event (ca. 0.3V) suggests the formation of at least one new species from the irreversible redox process.

Ruthenium complexes bearing the BQA ligand and 2,2′,2″-terpyridine (terpy) ligands were also examined to compare the BQA ligand's electron releasing character with its neutral terdentate counterpart. Thus, $[Ru(terpy)_2]^{2+}$ (**8**),[18] [(terpy)Ru(BQA)][BPh_4] (**9**), and Ru(BQA)$_2$ (**4**) were each studied by cyclic voltammetry. The mixed BQA/terpy complex **9** was readily synthesized by refluxing a dichloromethane solution of (terpy)$RuCl_2(PPh_3)$[19] with one equivalent of $NaBPh_4$ and **1** in the presence of three equivalents of triethylamine. The cyclic voltammograms for **8**, **9**, and **4** are presented in Figure 4a. The measurements were taken in 0.1 M ^{n}Bu$_4$NPF$_6$ in dichloromethane and referenced against an internal Fc/Fc$^+$ standard. Complexes **8**, **9**, and **4** (labeled A, B, and C in Figure 4a, respectively) each exhibit reversible waves assigned as $Ru^{III/II}$ couples. The effect of substituting the neutral terpy ligand by anionic BQA is dramatic. The $Ru^{III/II}$ couple shifts cathodically by ca. 620 mV from the dication **8** ($E_{1/2} = 0.92$ V)[18] to the monocation **9** ($E_{1/2} = 0.31$ V, $\Delta_p = 89$ mV); the $Ru^{III/II}$ couple shifts an additional 520 mV from **9** to neutral **4** ($E_{1/2} = -0.21$ V, $\Delta_p = 99$ mV). As for the iron derivative **2**, neutral **4** exhibits a second wave centered at $E_{1/2} = +0.60$ V ($\Delta_p = 97$ mV), though in this case, it exhibits a higher degree of reversibility. There is also a small feature, centered at ca. 0.3 V, that is most likely due to an impurity in the sample. As discussed above, the higher potential redox event may be attributable to a reversible $Ru^{IV/III}$ couple, or it may represent a redox event

(17) Connelly, N. G.; Geiger, W. E. *Chem. Rev.* **1996**, *96*, 877.

(18) Sauvage, J.-P.; Collin, J.-P.; Chambron, J.-C.; Guillerez, S.; Coudret, C.; Balzani, V.; Barigelletti, F.; De Cola, L.; Flamigni, L. *Chem. Rev.* **1994**, *94*, 993.

(19) Sullivan, B. P.; Calvert, J. M.; Meyer, T. J. *Inorg. Chem.* **1980**, *19*, 1404.

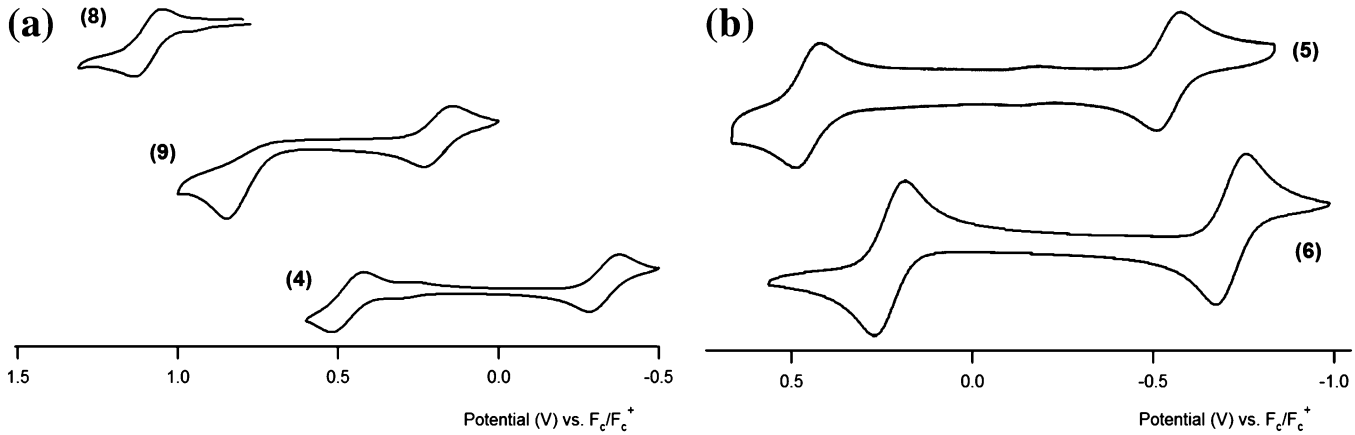

Figure 4. (a) Cyclic voltammetry of $[(terpy)_2Ru]^{2+}$ (**8**), $[(terpy)Ru(BQA)]^+$ (**9**), and $Ru(BQA)_2$ (**4**), in 0.4 M $^nBu_4NPF_6/CH_2Cl_2$, scan rate = 75 mV/s. (b) Cyclic voltammetry of (D) $(BQA)RuCl(PPh_3)_2$ (**5**) and (E) $(BQA)OsCl(PPh_3)_2$ (**6**), in 0.1 M $^nBu_4NPF_6/CH_2Cl_2$, scan rate = 50 mV/s.

Scheme 2

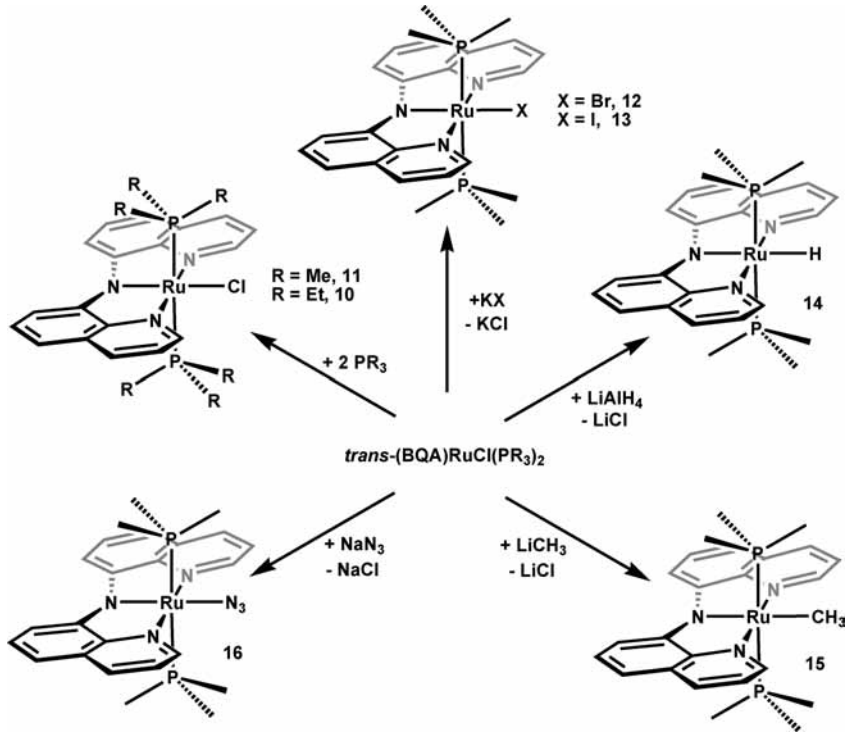

at the BQA ligand. At present, we cannot distinguish between these two possibilities, though it is noteworthy that the second redox wave is observed at significantly different potentials for the two $M(BQA)_2$ species (M = Fe, Ru).

The potential $M^{IV/III}$ redox couples observed for **2** and **4** prompted us to examine whether this feature was limited to complexes of the composition $M(BQA)_2$. Interestingly, both the ruthenium and osmium complexes, **5** and **6**, also exhibit two reversible redox processes, as shown in Figure 4b (0.4 M $^nBu_4NPF_6$ in dichloromethane, referenced to internal Fc/Fc^+). Complex **5** exhibits a reversible redox wave at $E_{1/2} = -0.55$ V ($\Delta_p = 78$ mV) assigned as the $Ru^{III/II}$ couple. The second reversible redox wave occurs at $E_{1/2} = +0.45$ V ($\Delta_p = 76$ mV). The Os complex **6** similarly displays two reversible redox processes centered at $E_{1/2} = -0.72$ V ($Os^{III/II}$, $\Delta_p = 85$ mV) and $E_{1/2} = +0.23$ V (BQA/BQA^+, $\Delta_p = 83$ mV).

Ligand Exchange Reactions. To survey the general reactivity of the $(BQA)MX(PPh_3)_2$ complexes, we probed exchange reactions of the phosphine and halide ligands (Scheme 2). Substitution of the PPh_3 units on **5** for smaller, stronger σ-donor phosphine ligands occurs under relatively mild conditions. For example, triethylphosphine fully substitutes in refluxing toluene to form *trans*-$(BQA)RuCl(PEt_3)_2$ (**10**), while trimethylphosphine fully substitutes at room temperature to form *trans*-$(BQA)RuCl(PMe_3)_2$ (**11**) (Scheme 2). The trans geometry is preserved as evidenced by the ^{31}P NMR spectrum, which shows a single chemical shift for both **10** and **11** at 11.8 and 0.5 ppm, respectively. Refluxing **5** in excess pyridine resulted in incomplete phosphine substitution, as ascertained by ^{31}P NMR, while acetonitrile did not effect any phosphine displacement under refluxing conditions. Likewise, refluxing precursor **5** with larger ligand types such as PCy_3 failed to afford phosphine displacement.

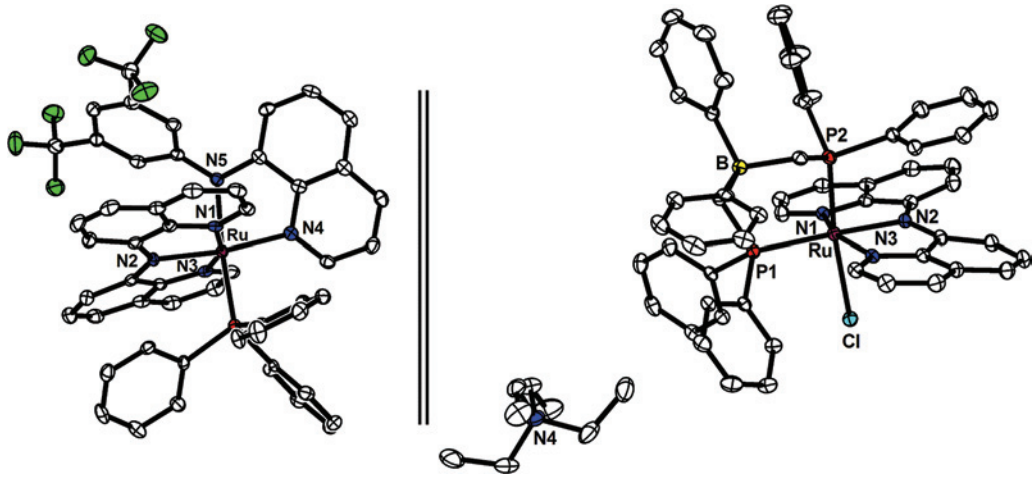

Figure 5. Displacement ellipsoid representation (50%) of (left) (BQA)Ru(3,5-$(CF_3)_2$-(C_6H_3)QA)(PPh_3) (**19**) and (right) [(Ph_2BP_2)RuCl(BQA)][NEt_4] (**21**). Hydrogen atoms and solvent molecules have been removed for clarity. Selected bond distances (Å) and angles (deg) for **19**: Ru−N1 2.066(3), Ru−N2 2.021(3), Ru−N3 2.045(3), Ru−N4 2.094(3), Ru−N5 2.144(3), Ru−P1 2.319(1), N1−Ru−N2 81.02(1), N2−Ru−N3 80.88(1), N1−Ru−N3 160.82(1), N4−Ru−N5 77.48(1), N5−Ru−P1 170.99(1). For **21**: Ru−N1 2.095(4), Ru−N2 2.050(4), Ru−N3 2.078(4), Ru−Cl 2.515(1), Ru−P1 2.353(1), Ru−P2 2.291(1), N1−Ru−N2 78.9(1), N2−Ru−N3 79.8(1), N1−Ru−N3 158.1(1), P1−Ru−P2 90.33(5).

Scheme 3

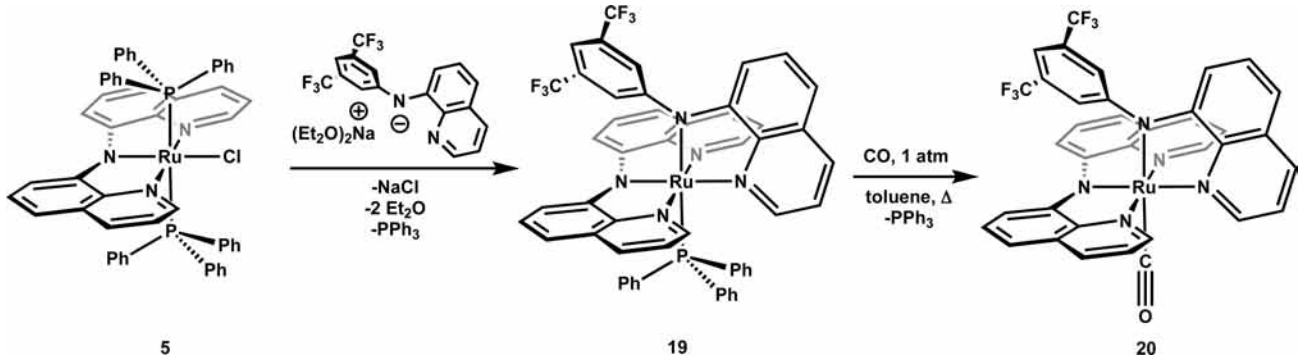

We also probed the replacement of the halide ligand in **11** with several other anionic ligands. For instance, refluxing **11** in THF with four equivalents of potassium halide salts produced the bromide and iodide complexes *trans*-(BQA)Ru-Br(PMe_3)$_2$ (**12**) and *trans*-(BQA)RuI(PMe_3)$_2$ (**13**) (Scheme 2). The reaction between **11** and $LiAlH_4$ in toluene at room temperature provided the hydride complex *trans*-(BQA)Ru-H(PMe_3)$_2$ (**14**) in moderate yield. Access to the methyl complex *trans*-(BQA)RuMe(PMe_3)$_2$ (**15**) required excess MeLi in refluxing toluene. The azide complex *trans*-(BQA)Ru(N_3)(PMe_3)$_2$ (**16**) was readily prepared by refluxing NaN_3 and **11** in a mixture of THF and dichloromethane for several hours. Complexes **12**−**16** all maintain the coordination environment of the parent species **11**, showing no propensity to give rise to other isomers. For the methyl and hydride derivatives in particular, it is noteworthy that the amido N atom and the alkyl/hydride ligand remain trans-disposed. This contrasts with PCP-type pincer systems, where cis disposition is often favored.[20] We presume that the amido N atom of the BQA system is not very strongly trans influencing, and that the phosphine ligands themselves are appreciably more so.

We also canvassed the reaction between **5** and the sodium salt of the bidentate monoquinolinyl-amide ligand [3,5-$(CF_3)_2$-(C_6H_3)QA][Na(Et_2O)] (**18**), because we were interested in determining whether the two amide functionalities would adopt a cis or trans arrangement. This reaction produced the deep purple complex (BQA)Ru(3,5-$(CF_3)_2$-(C_6H_3)QA)(PPh_3) (**19**) (Scheme 3). For **19**, the amide from the monoquinoline ligand adopts a trans disposition to the phosphine ligand, orienting the bulky bis-3,5-triflouromethyl phenyl amide substituent on the opposite side of the BQA plane from the phosphine ligand. This orientation was verified via crystallographic characterization of **19**, whose solid-state structure is shown in Figure 5, and can likely be explained on steric grounds alone. Interestingly, the monoquinolinyl amido N atom that is trans to the phosphine ligand (N5 in Figure 5) is substantially elongated relative to the amido N atom from the BQA ligand (N2 in Figure 5) due to the strong trans influence of the phosphine ligand. Substitution of the remaining phosphine ligand of **19** occurs when it was refluxed in toluene. For example, the carbonyl adduct (BQA-)Ru(3,5-$(CF_3)_2$-(C_6H_3)QA)(CO) (**20**) is formed by refluxing **19** in toluene under an atmosphere of CO gas for 20 h. Formation of **20** from **19** is accompanied by a color change from deep purple to an intense red.

(20) (a) Vila, J. M.; Pereira, M. T.; Ortigueira, J. M.; Lata, D.; Lopez Torres, M.; Fernandez, J. J.; Fernandez, A.; Adams, H. *J. Organomet. Chem.* **1998**, *566*, 93. (b) Crespo, M.; Solans, X.; Font-Bardia, M. *Polyhedron* **1998**, *17*, 3927. (c) Gandelman Vigalok, A.; Shimon, L. J. W.; Milstein, D. *Organometallics* **1997**, *16*, 3981.

Scheme 4

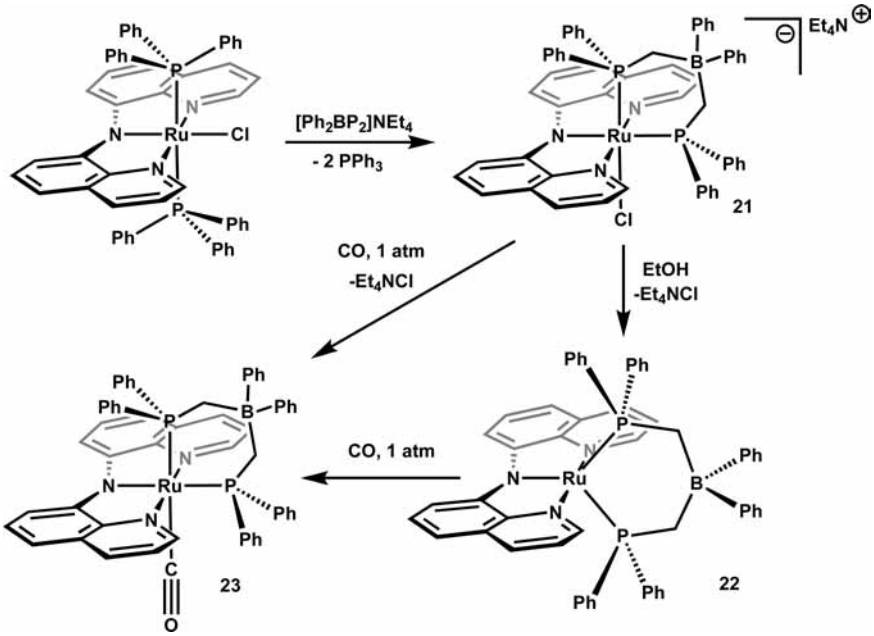

Scheme 5

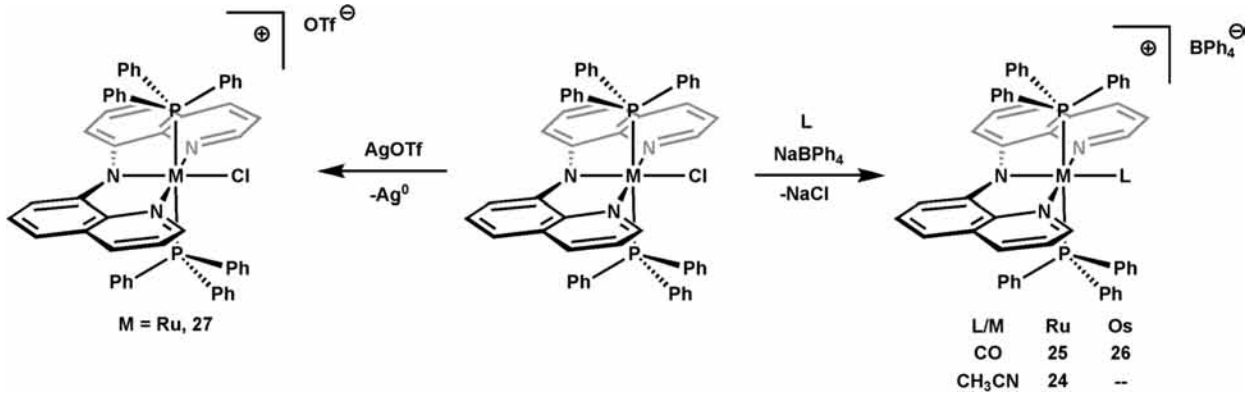

The reaction of **5** with the anionic bis(phosphine) ligand $[Ph_2B(CH_2PPh_2)_2][NEt_4]$ (hereafter referred to as $[Ph_2BP_2]$)[21] in THF generated the product $\{[Ph_2BP_2]RuCl(BQA)\}\{NEt_4\}$ (**21**) as a midnight blue solid. The ^{31}P NMR spectrum for complex **21** displays a doublet of doublets (δ 54, 28.3 ppm, $^2J_{P-P}$ = 36 Hz), indicating the inequivalent phosphorus environments. This is confirmed by the solid-state X-ray crystal structure (Figure 5). The $[Ph_2BP_2]^-$ ligand afforded complete displacement of the phosphine ligands from **5**. Interestingly, the chloride remains coordinated to the metal in a position cis to the amido nitrogen. Washing **21** with ethanol, however, extracts NEt_4Cl to precipitate the 16-electron, neutral complex $[Ph_2BP_2]Ru(BQA)$ (**22**) as a wine red solid (Scheme 4). Complex **22** displays a singlet in its ^{31}P NMR spectrum at 69 ppm, which suggests that the phosphine positions are equivalent on the NMR time scale, and we presume **22** adopts the trigonal-bipyramidal geometry shown in Scheme 4, though no solid-state structural data are available. The neutral complex **22** is stable as a coordinatively unsaturated complex and does not bind an equivalent of dinitrogen, even under elevated pressures (60−80 psi). This was somewhat surprising to us, especially in light of observations regarding N_2 binding described below. The carbonyl complex $[Ph_2BP_2]Ru(CO)(BQA)$ (**23**) can be readily prepared, however, by the addition of CO gas to a solution of **22** in dichloromethane, or alternatively, by chloride displacement in **21** in THF.

Cationic (BQA)M(PR$_3$)$_2$(L)$^+$ Species (M = Ru, Os). Halide abstraction routes were also canvassed so as to expose a labile coordination site at the $(BQA)M(PR_3)_2(X)$ species. Chloride abstraction reactions with **5** or **6** using sodium or potassium reagents such as $NaBPh_4$ or KPF_6 proceeded only in the presence of relatively good donor solvents. For instance, the reaction of *trans*-$(BQA)RuCl(PPh_3)_2$ (**5**) with $NaBPh_4$ in a mixture of THF/acetonitrile immediately produced the purple solvento species $[(BQA)Ru(NCCH_3)(PPh_3)_2][BPh_4]$ (**24**) with a concomitant release of NaCl (Scheme 5). By contrast, complex **5** is not reactive toward an excess of $NaBPh_4$ under a dinitrogen atmosphere over a period of several days, even when pressurized with N_2 (14−80 psi of N_2). This was true in a variety of solvents

(21) Thomas, J. C.; Peters, J. C. *J. Am. Chem. Soc.* **2001**, *123*, 5100.

Scheme 6

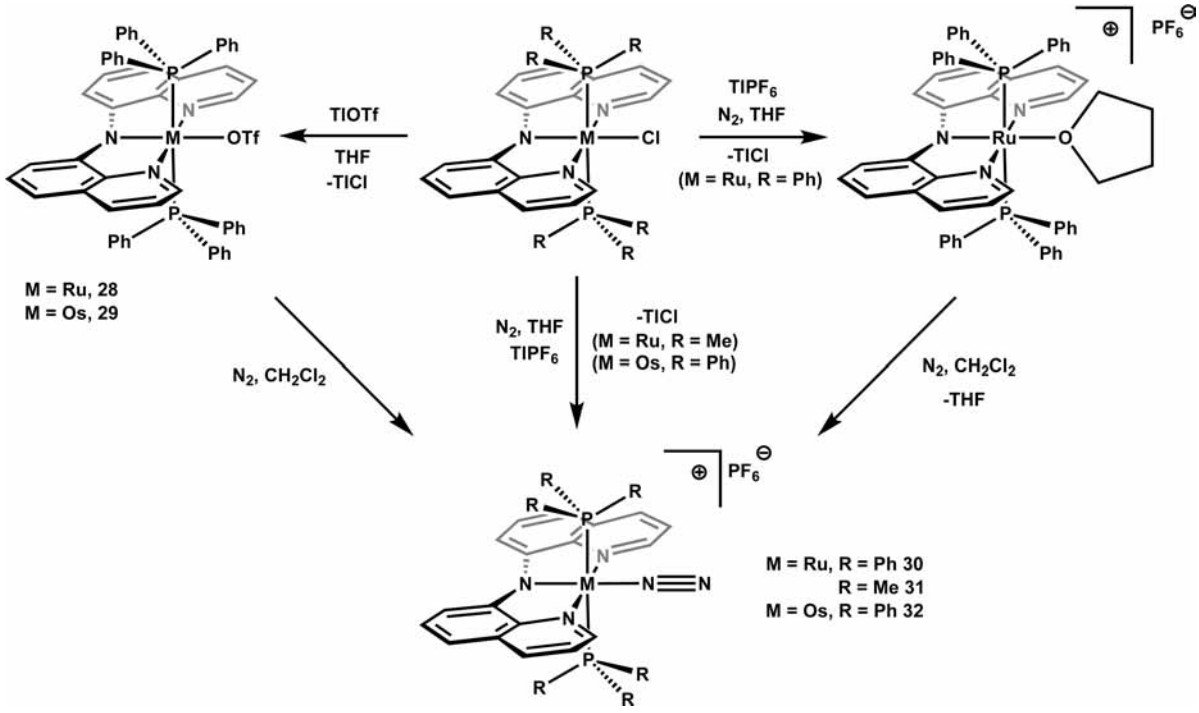

(e.g., THF, THF/EtOH, CH_2Cl_2). The reaction of **5** with $NaBPh_4$ under an atmosphere of carbon monoxide in THF produces the cherry red complex $[(BQA)Ru(CO)(PPh_3)_2][BPh_4]$ (**25**) within minutes (Scheme 5). The Os congener $[(BQA)Os(CO)(PPh_3)_2][BPh_4]$ (**26**) can be similarly synthesized from **6** and $NaBPh_4$. For both **25** and **26**, the phosphines remain trans-disposed, as indicated by their ^{31}P NMR spectra, which show single peaks for both species ($\delta = 30.1$ ppm for **25**, 0.31 ppm for **26**). The infrared stretching frequency of the carbonyl ligand for cationic **25** ($\nu_{CO} = 1946\ cm^{-1}$) is lower than that of the neutral terpyridine complex $(trpy)RuCl_2(CO)$ ($\nu_{CO} = 1953\ cm^{-1}$).[19] The Os complex **26** features a more substantially reduced carbonyl stretching frequency ($\nu_{CO} = 1921\ cm^{-1}$) from **25**.

In an effort to realize Ru(BQA) systems that might bind dinitrogen, more aggressive halide scavenging reagents were canvassed. Puenta and co-workers successfully employed AgOTf as a halide scavenger to form a cationic dinitrogen complex en route to $[TpRu(N_2)(PEt_3)_2][BPh_4]$ (Tp = hydrotris(pyrazolyl)borate),[22] and van Koten et al. have reported that the PCP-pincer complex $[Ru^{II}(OTf)\{C_6H_2(CH_2PPh_2)_2\}(PPh_3)]$ can be prepared by the addition of AgOTf to the corresponding chloride precursor.[23] However, when a solution of **5** in THF protected from ambient room light is exposed to an equimolar amount of AgOTf, the initially aqua-blue hue of **5** immediately fades along with the production of a dark brown precipitate and Ag^0 mirror. The isolated brown solid is assigned as the paramagnetic oxidation product $[(BQA)Ru^{III}Cl(PPh_3)_2][OTf]$ (**27**) (Scheme 5).

To circumvent a metal oxidation event, thallium reagents were employed. The divalent triflate complexes $(BQA)Ru(OTf)(PPh_3)_2$ (**28**) and $(BQA)Os(OTf)(PPh_3)_2$ (**29**) thus proved available by reaction between the corresponding chloride complexes **5** and **6** and TlOTf in THF (Scheme 6). These complexes are difficult to isolate in analytically pure form, presumably due to the high lability of the triflate ligand and propensity to coordinate solvent or dinitrogen. Thus, when **5** is stirred with $TlPF_6$ in THF solution, the color of the solution darkens within minutes to produce a midnight blue solution along with concurrent release of a white precipitate. A ^{31}P NMR spectrum of this solution, taken in situ, shows a very modest shift from **5** ($\delta = 29$ ppm) to 28 ppm, whereas the solution IR does not reveal any vibrations unique from the parent species **5**. We therefore conclude that this species is the THF solvent adduct $[(BQA)Ru(THF)(PPh_3)_2][PF_6]$. Removal of the reaction volatiles in vacuo yields a purple solid that has limited solubility in THF and is completely insoluble in hydrocarbon solvents (e.g., pentane, benzene, toluene). Dissolution of this purple residue in dichloromethane affords an intense cherry-red solution ($\lambda_{max} = 542$ nm), and examination of its IR spectrum reveals an intense vibration at 2130 cm^{-1} attributable to a coordinated dinitrogen ligand. The product is thus assigned as *trans*-$[(BQA)Ru(N_2)(PPh_3)_2][PF_6]$ (**30**). Complex **30** shows a single ^{31}P NMR resonance at 25 ppm, confirming that the phosphines remain trans-disposed. The THF adduct complex has not been more thoroughly characterized due to its propensity to form **30** upon storage under N_2 atmospheres.

Thallium halide abstraction from the more electron-rich PMe_3 complex **11** with $TlPF_6$ proceeds directly to the dinitrogen adduct complex $[(BQA)Ru(N_2)(PMe_3)_2][PF_6]$ (**31**) in THF solutions (KBr/THF; $\nu_{NN} = 2129\ cm^{-1}$), without

(22) Tenorio, M. A. J.; Tenorio, M. J.; Puerta, M. C.; Valerga, P. *J. Chem. Soc., Dalton Trans.* **1998**, 3601.
(23) Karlen, T.; Dani, P.; Grove, D. M.; Steenwinkel, P.; van Koten, G. *Organometallics* **1996**, *15*, 5687.

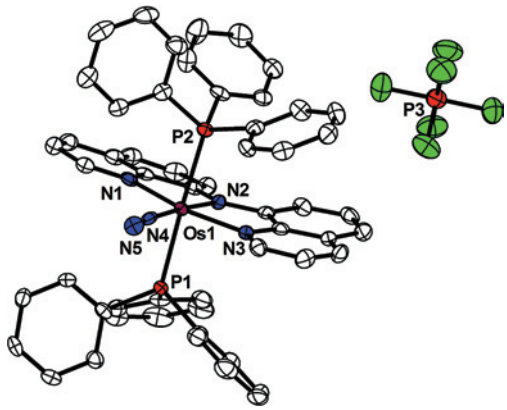

Figure 6. Displacement ellipsoid representation (50%) of $[(BQA)Os(N_2)(PPh_3)_2][PF_6]$ (**32**). Hydrogen atoms have been removed for clarity. Selected bond distances (Å) and angles (deg) for **32**: Os−N1 2.096(2), Os−N2 2.032(3), Os−N3 2.062(2), Os−N4 1.954(3), N4−N5 1.080(4), Os−P1 2.403(1), Os−P2 2.403(1), N1−Os−N2 79.97(1), N2−Os−N3 80.80(1), N1−Os−N3 160.6(1), P1−Os−P2 177.4(1).

discernible formation of a THF solvent adduct species. Likewise, reaction of the Os complex **6** with $TlPF_6$ produces the dinitrogen adduct $[(BQA)Os(N_2)(PPh_3)_2][PF_6]$ (**32**) without an observable THF solvent adduct precursor (see Scheme 6). The Os congener **32** is appreciably more stable than its ruthenium cousins and is identifiable as the Os−N_2 cation by ES-MS ($m/z = 1014$) and IR spectroscopy ($\nu_{NN} = 2073$ cm^{-1}). A solid-state crystal structure of this latter species was obtained via XRD analysis, further confirming that the N_2 ligand resides at the site trans to the amido nitrogen (Figure 6). The dinitrogen ligand does not exhibit significant elongation from free N_2.[24]

Conclusions

The bis(quinolinyl)amido ligand featured in this manuscript can be exploited as an anionic analogue of the ubiquitous, neutral polypyridine ligand 2,2′,2″-terpyridine (terpy). The family of Ru and Os complexes described herein underscores this point. Comparative electrochemical studies establish that the bis(quinolinyl)amido ligand substantially shifts $M^{III/II}$ and $M^{IV/III}$ redox couples cathodically relative to structurally related terpy derivatives. We caution that the degree to which the BQA ligand can behave as a redox noninnocent ligand has yet to be firmly established. Hence ligand-centered oxidation cannot be ruled out at positive potentials. Regardless, the $(BQA)M^{II}(L)_2$ platform (M = Ru, Os) gives rise to a wealth of well-defined substitution chemistry providing access to a structurally diverse set of complexes. Opportunities for small molecule activation chemistry within these systems are envisaged. The N_2 adducts characterized herein suggest that favorable π-donation from the BQA ligand will facilitate binding of π-acidic substrates at the site trans to the N-amido donor. Future studies will aim to explore the reactivity patterns of the systems described herein.

(24) Stoicheff, B. P *Can. J. Phys.* **1954**, *82*, 630.

Experimental Section

All manipulations were carried out using standard Schlenk or glovebox techniques under a dinitrogen atmosphere. Unless otherwise noted, solvents were deoxygenated and dried by thorough sparging with N_2 gas followed by passage through an activated alumina column. Nonhalogenated solvents were typically tested with a standard purple solution of sodium benzophenone ketyl in tetrahydrofuran in order to confirm effective oxygen and moisture removal. The reagents $NaBPh_4$, $TlPF_6$, $FeCl_2$, and $FeCl_3$(anhydrous) were purchased from commercial vendors and used without further purification. HBQA (**1**, HBQA = bis(quinolinyl)amide),[1] $RuCl_2(PPh_3)_3$,[25] $[RuCl_2(cod)]_n$,[26] $OsCl_2(PPh_3)_3$,[27] and $[Ph_2B(CH_2PPh_2)_2][NEt_4]$[21] were synthesized as described previously. Deuterated solvents were degassed and stored over activated 3 Å molecular sieves prior to use. Elemental analyses were carried out at Desert Analytics, Tucson, Arizona. NMR spectra were recorded at ambient temperature on Varian Mercury 300 MHz, Joel 400 MHz, and Anova 500 MHz spectrometers, unless otherwise noted. ^1H and ^{13}C NMR chemical shifts were referenced to residual solvent. ^{31}P NMR, ^{11}B NMR, and ^{19}F NMR chemical shifts are reported relative to an external standard of 85% H_3PO_4, neat $BF_3 \cdot Et_2O$, and neat $CFCl_3$, respectively. IR spectra were recorded on a Bio-Rad Excalibur FTS 3000 spectrometer controlled by Win-IR Pro software. MS data for samples were obtained by injection of a hydrocarbon solution into a Hewlett-Packard 1100MSD Mass Spectrometer (ES^+) or an Agilent 5973 Mass Selective Detector (EI). UV−vis measurements were taken on a Hewlett-Packard 8452A diode array spectrometer using a quartz crystal cell with a Teflon cap. X-ray diffraction studies were carried out in the Beckman Institute Crystallographic Facility on a Bruker Smart 1000 CCD diffractometer.

X-Ray Crystallography Procedures. X-ray-quality crystals were grown as indicated in the experimental procedures for each complex. The crystals were mounted on a glass fiber with Paratone-N oil. Structures were determined using direct methods with standard Fourier techniques using the Bruker AXS software package. In some cases, Patterson maps were used in place of the direct methods procedure.

EPR Measurements. X-band EPR spectra were obtained on a Bruker EMX spectrometer equipped with a rectangular cavity working in the TE_{102} mode. Variable-temperature measurements were conducted with an Oxford continuous-flow helium cryostat (temperature range 3.6−300 K). Accurate frequency values were provided by a frequency counter built in the microwave bridge. Solution spectra were acquired in toluene for all of the complexes. Sample preparation was performed under a nitrogen atmosphere.

$[Fe(BQA)_2][BPh_4]$ (2). HBQA and (0.82 g, 3.02 mmol) and $FeCl_3$ (anhydrous) (245 mg, 1.5 mmol) were added to a flask and stirred in CH_2Cl_2 (25 mL). A solution of Na_2CO_3 (320 mg, 3.05 mmol) and $NaBPh_4$ (517 mg, 1.5 mmol) in H_2O (30 mL) was then added to this slurry. The reaction mixture was stirred for 20 h at room temperature. The product was extracted into CH_2Cl_2 and washed with H_2O (3 × 25 mL). The organic phase was evaporated to dryness to yield a red powder (0.98 g, 71%). ^1H NMR (DMSO-d_6, 300 MHz, 25 °C): δ 29.1, 19.8, 7.17, 6.91 (t, J = 6.6 Hz), 6.77 (t, J = 6.6 Hz), −8.3, −29.0, −61.7, −65.3. UV−vis [λ_{max}/nm (ε/M^{-1} cm^{-1})]: 1030 (11 000), 680 (2700), 514 (33 000), 418 (49 000), 306 (90 000). ES-MS (electrospray): positive mode

(25) Hallman, P. S.; Stephenson, T. A.; Wilkinson, G. *Inorg. Synth.* **1970**, *12*, 237.
(26) Bennett, M. A.; Smith, A. K. *J. Chem. Soc., Dalton Trans.* **1974**, 233.
(27) Elliott, G. P.; McAuley, N. M.; Roper, W. R. *Inorg. Synth.* **1989**, *26*, 184.

$[(BQA)_2Fe]^+$ *m*/*z* 596, found $(M)^+$ *m*/*z* 596; $[Ph_4B]^-$ *m*/*z* 319, found $(M)^-$ *m*/*z* 319. Anal. calcd for $C_{60}H_{44}BFeN_6$: C, 75.45; H, 4.58; N, 11.12. Found: C, 75.22; H, 4.68; N, 11.00.

(BQA)RuCl(cod) (3). A suspension of $Ru(cod)Cl_2$ (0.36 g, 1.3 mmol) in toluene (10 mL) was treated with a solution of [BQA][Li] (0.35 g, 1.3 mmol) in toluene (10 mL) at room temperature. After the mixture was stirred for 48 h, the solvent was removed in vacuo. The residue was extracted with dichloromethane and filtered through Celite on a sintered glass frit to yield a purple filtrate. Layering the filtrate with petroleum ether precipitated a purple solid. The product was collected via filtration, washed with copious amounts of petroleum ether, and dried in vacuo (0.41 g, 62%). ^{1}H NMR ($CDCl_3$, 300 MHz): δ 9.12−9.11 (m, 2H), 8.12−8.09 (m, 2H), 7.90−7.87 (m, 2H), 7.48−7.37 (m, 2H), 7.01−6.98 (m, 2H), 4.52−4.50 (m, 2H), 3.19−3.17 (m, 2H), 2.67−2.60 (m 2H), 2.29−2.20 (m, 2H), 1.96−1.92 (m, 2H), 1.80−1.74 (m, 2H). ^{13}C $\{^1$H$\}$ NMR ($CDCl_3$, 75 MHz): δ 149.94, 137.14, 131.68, 128.83, 128.42, 122.60, 122.03, 113.52, 112.85, 94.75, 89.92, 30.39, 28.68. UV−vis [λ_{max}/nm (ε/M^{-1} cm^{-1})]: 324 (9900), 302 (7000), 590 (6200). Anal. calcd for $C_{26}H_{24}ClN_3Ru$: C, 60.64; H, 4.70; N, 8.16. Found: C, 60.73; H, 4.82; N, 7.89.

Ru(BQA)$_2$ (4). A suspension of $Ru(cod)Cl_2$ (0.36 g, 1.3 mmol) in toluene (10 mL) was added to a solution of [BQA][Li] (0.72 g, 2.6 mmol) in toluene (10 mL) in a bomb reactor with a Teflon stopcock. The mixture was heated at reflux for 48 h. The volatiles were removed in vacuo, and the residue was extracted with dichloromethane and filtered through Celite on a sintered glass frit to yield a red-purple filtrate. Layering the filtrate with petroleum ether precipitated a burgundy solid. The product was collected via filtration, washed with copious amounts of petroleum ether, and dried in vacuo (0.83 g, 89%). ^{1}H NMR (CD_2Cl_2, 300 MHz, 25 °C): δ 9.10 (dd, J = 4.8 Hz, 1.5 Hz, 4H), 7.16 (d, J = 7.8 Hz, 4H), 7.05 (m, J = 8.1 Hz, 4H), 6.65 (m, J = 7.8 Hz, 8H), 6.35 (dd, J = 4.8 Hz, 1.5 Hz, 4H). ^{13}C $\{^1$H$\}$ NMR (CD_2Cl_2, 75 MHz): δ 150, 138, 132, 129, 128.4, 122.8, 122. Anal. calcd for $C_{36}H_{24}N_6Ru$: C, 67.38; H, 3.77; N, 13.10. Found: C, 67.63; H, 3.66; N, 13.12.

***trans*-(BQA)RuCl(PPh$_3$)$_2$ (5).** A solution of HBQA (500 mg, 1.84 mmol) and NEt_3 (373 mg, 3.69 mmol) in CH_2Cl_2 (5 mL) was added to a stirring solution of $RuCl_2(PPh_3)_4$ (2.25 g, 1.84 mmol) in CH_2Cl_2 (8 mL). The reaction solution was heated to 65 °C for 5 h. The reaction was then cooled to room temperature and the solvent removed in vacuo. The green solid was washed with ethanol (2 × 15 mL), Et_2O (2 × 15 mL), and petroleum ether (2 × 15 mL). The remaining solid was dried in vacuo, yielding 1.21 g of **5** (70.2%). Crystals of $(BQA)RuCl(PPh_3)_2$ were grown by vapor diffusion of petroleum ether into benzene. ^{1}H NMR (C_6D_6, 300 MHz, 25 °C): δ 9.036 (dd, J = 4.8 Hz, 1.5 Hz, 2H), 7.49 (m, 12H), 7.08 (d, J = 7.8 Hz, 2H), 6.96 (t, J = 8.1 Hz, 2H), 6.75−6.87 (m, 20 H), 6.53 (d, J = 7.8 Hz, 4H), 6.40 (dd, J = 4.8 Hz, 1.5 Hz, 4H). ^{31}P $\{^1$H$\}$ NMR (C_6D_6, 121.4 MHz, 25 °C): δ 29.2. ES-MS (electrospray): calcd for $C_{54}H_{42}ClN_3P_2Ru$ $(M)^-$ *m*/*z* 931, found (M + H) *m*/*z* 931, 669 (M − PPh_3). Anal. calcd for $C_{54}H_{42}ClN_3P_2Ru$: C, 69.63; H, 4.55; N, 4.51. Found: C, 68.93; H, 4.69; N, 4.49.

***trans*-(BQA)OsCl(PPh$_3$)$_2$ (6).** A solution of [BQA][Li] (300 mg, 1.11 mmol) in toluene (5 mL) was added to a stirring solution of $OsCl_2(PPh_3)_4$ (1.156 g, 1.11 mmol) in toluene (8 mL) at room temperature. The reaction solution was heated to 65 °C for 5 h. The reaction was then cooled to room temperature, and the volatiles were removed in vacuo. The green solid was washed with ethanol (2 × 15 mL), Et_2O (2 × 15 mL), and petroleum ether (2 × 15 mL). The remaining solid was dried in vacuo, yielding 1.04 g of analytically pure material (92%). Crystals of **6** were grown by vapor diffusion of petroleum ether into benzene. ^{1}H NMR (CD_2Cl_2, 300 MHz, 25 °C): δ 8.44 (dd, J = 4.8 Hz, 1.5 Hz, 2H), 7.62 (m, 12H), 7.08 (d, J = 7.8 Hz, 2H), 6.94 (t, J = 8.2 Hz, 2H), 6.75−6.87 (m, 20 H), 6.48 (d, J = 7.8 Hz, 4H), 6.38 (dd, J = 4.8 Hz, 1.5 Hz, 4H). ^{31}P $\{^1$H$\}$ NMR (C_6D_6, 121.4 MHz, 25 °C): δ −8. ES-MS (electrospray): calcd for $C_{54}H_{42}ClN_3P_2Os$ (M) *m*/*z* 1020, found (M + H) *m*/*z* 1021, 986 (M − Cl). Anal. calcd for $C_{54}H_{42}ClN_3P_2Os$: C, 63.55; H, 4.15; Cl, 3.47; N, 4.12. Found: C, 63.46; H, 4.02; N, 4.10.

***cis*-(BQA)OsCl(PPh$_3$)$_2$ (7).** A solution of HBQA (500 mg, 1.84 mmol) and NEt_3 (373 mg, 3.69 mmol) in CH_2Cl_2 (5 mL) was added to a stirring solution of $OsCl_2(PPh_3)_3$ (1.93 g, 1.84 mmol) in CH_2Cl_2 (8 mL). The reaction solution was heated to 65 °C for 5 h. The reaction was then cooled to room temperature, and the volatiles were removed in vacuo. The brown solid was washed with ethanol (2 × 15 mL), Et_2O (2 × 15 mL), and petroleum ether (2 × 15 mL). The remaining solid was dried in vacuo, yielding 1.26 g of **7** (67%). Vapor diffusion of petroleum ether into a solution of **7** in benzene yielded crystals of the trans product **6**. ^{1}H NMR (C_6D_6, 300 MHz, 25 °C): δ 8.8 (dd, J = 4.8 Hz, 1.5 Hz, 2H), 7.6−6.5 (m, 36 H), 6.40 (dd, J = 4.8 Hz, 1.5 Hz, 4H). ^{31}P $\{^1$H$\}$ NMR (C_6D_6, 121.4 MHz, 25 °C): δ 2.2 (d, J = 10.7 Hz), −0.92 (d, J = 10.7 Hz). ES-MS (electrospray): calcd for $C_{54}H_{42}ClN_3P_2Os$ $(M)^+$ *m*/*z* 1020, found (M + H) *m*/*z* 1021, 986 (M − Cl).

[(terpy)Ru(BQA)][BPh$_4$] (9). A solution of HBQA (32.6 mg, 0.12 mmol) and NEt_3 (30 mg, 0.37 mmol) in CH_2Cl_2 (5 mL) was added to a stirring solution of $(tpy)RuCl_2(PPh_3)$ (50 mg, 0.075 mmol) and $NaBPh_4$ (15 mg, 0.075 mmol) in ethanol (5 mL) at room temperature. The reaction solution was then heated at 65 °C for 15 h. The reaction mixture was then cooled to room temperature, and the volatiles were removed in vacuo. The red solid was washed with Et_2O (2 × 15 mL) and petroleum ether (2 × 15 mL). The remaining solid was dried in vacuo, yielding 59.6 mg of analytically pure material (86%). ES-MS (electrospray): calcd for $C_{33}H_{23}N_6Ru$ $(M)^+$ *m*/*z* 605, found (M^+) *m*/*z* 605. Anal. calcd for $C_{57}H_{43}BN_6Ru$: C, 74.10; H, 4.69; N, 9.10. Found: C, 74.35; H, 4.75; N, 9.06.

***trans*-(BQA)RuCl(PEt$_3$)$_2$ (10).** A blue solution of **5** (0.15 g, 0.47 mmol) in toluene (10 mL) was treated with neat triethylphosphine (0.20 mL, 2.0 mmol) at room temperature. The mixture was heated to reflux for 18 h. The reaction mixture was cooled down, and all volatile materials were removed in vacuo. The green solids were washed with Et_2O (3 × 15 mL) and petroleum ether (3 × 15 mL). The remaining green solid was dried in vacuo to yield analytically pure material (0.073 g, 70%). ^{1}H NMR (C_6D_6, 300 MHz): δ 9.06 (dd, J = 4.8 Hz, 1.5 Hz, 4H), 7.18 (d, J = 7.8 Hz, 4H), 7.04 (t, J = 8.2 Hz, 4H), 6.72 (d, J = 7.8 Hz, 8H), 6.40 (dd, J = 4.8 Hz, 1.5 Hz, 4H), 1.82 (m, 12 H), 0.70 (d, 18H). ^{31}P$\{^1$H$\}$ NMR (C_6D_6, 121 MHz) δ 11.8. Anal. calcd for $C_{30}H_{42}ClN_3P_2Ru$: C, 56.02; H, 6.58; N, 6.53. Found: C, 55.88; H, 6.48; N, 6.51.

***trans*-(BQA)RuCl(PMe$_3$)$_2$ (11).** A blue solution of **5** (0.44 g, 0.47 mmol) in THF (10 mL) was treated with neat trimethylphosphine (0.19 mL, 1.9 mmol) at −30 °C. The mixture was allowed to warm to room temperature, and during that time, the solution turned green. After the mixture was stirred at room temperature for 1 h, all volatile materials were removed in vacuo. Flash column chromatography with 4:1 toluene/ethyl acetate yielded a black purple analytically pure solid (0.18 g, 69%) (R_f = 0.21). ^{1}H NMR (C_6D_6, 300 MHz): δ 9.06−9.03 (m, 2H), 7.70−7.67 (m, 2H), 7.34−7.22 (m, 4H), 6.74−6.72 (m, 2H), 6.58−6.53 (m, 2H), 0.68 (t, J = 3.0 Hz, 18H). ^{13}C$\{^1$H$\}$ NMR (C_6D_6, 75 MHz): δ 152.56, 151.74, 148.27 (t, J = 2.4 Hz), 132.32 (t, J = 1.7 Hz), 131.78, 128.14, 121.94, (t, J = 1.6 Hz), 113.69, 113.36, 11.03 (t, J = 11.3 Hz). ^{31}P$\{^1$H$\}$ NMR (C_6D_6, 121 MHz): δ 0.47. ES-MS (electro-

spray): calcd for $C_{24}H_{30}ClN_3P_2Ru$ $(M)^+$ *m/z* 559, found (M^+) *m/z* 559. Anal. calcd for $C_{24}H_{30}ClN_3P_2Ru$: C, 51.57; H, 5.41; N, 7.52. Found: C, 51.66; H, 5.35; N, 7.43.

***trans*-(BQA)RuBr(PMe$_3$)$_2$ (12).** A green solution of **11** (0.13 g, 0.23 mmol) in 4 mL of THF/MeOH (1:1) was mixed with potassium bromide (90 mg, 0.76 mmol) at room temperature. The mixture was heated to 50 °C for 4 h, cooled, and filtered over a pad of Celite. The filtrate was dried in vacuo, then redissolved in toluene and flashed through silica gel. The volatiles were removed in vacuo to yield a purple solid. The purple product was washed with petroleum ether (2 × 15 mL) and dried in vacuo (0.11 g, 77%). ^{1}H NMR (C_6D_6, 300 MHz): δ 9.19−9.17 (m, 2H), 7.70−7.67 (m, 2H), 7.30−7.22 (m, 4H), 6.73−6.70 (m, 2H), 6.53−6.48 (m, 2H), 0.72 (t, J = 3.0 Hz, 18H). ^{13}C{^{1}H} NMR (C_6D_6, 75 MHz): δ 152.02, 151.52, 149.72 (t, J = 2.3 Hz), 132.42, 131.68, 128.12, 122.02, 113.66, 113.41, 11.54 (t, J = 11.5 Hz). ^{31}P{^{1}H } NMR (C_6D_6, 121 MHz): δ −0.94. Anal. calcd for $C_{24}H_{30}BrN_3P_2Ru$: C, 47.77; H, 5.01; N, 6.96. Found: C, 50.72; H, 5.30; N, 6.50.

***trans*-(BQA)RuI(PMe$_3$)$_2$ (13).** A green solution of **11** (89 mg, 0.16 mmol) in 4 mL of THF/MeOH (1:1) was mixed with potassium iodide (90 mg. 0.54 mmol) at room temperature. The mixture was heated at 50 °C for 4 h, filtered over a pad of Celite, and the volatiles removed in vacuo to yield a purple solid. The filtrate was dried in vacuo, then redissolved in toluene and flashed through silica gel. Removal of the volatiles in vacuo afforded analytically pure material (87 mg, 84%). ^{1}H NMR (C_6D_6, 300 MHz): δ 9.38−9.35 (m, 2H), 7.71−7.68 (m, 2H), 7.28−7.22 (m, 4H), 6.70−6.68 (m, 2H), 6.46−6.41 (m, 2H), 0.79 (t, J = 3.0 Hz, 18H). ^{13}C{^{1}H } NMR (C_6D_6, 75 MHz): δ 152.59 (m), 151.50, 150.73, 132.75, 131.79, 128.30, 122.32, 113.82, 113.65, 12.83 (t, J = 11.9 Hz). ^{31}P{^{1}H } NMR (C_6D_6, 121 MHz): δ −2.96. Anal. calcd for $C_{24}H_{30}IN_3P_2Ru$: C, 44.32; H, 4.65; N, 6.46. Found: C, 44.32; H, 4.70; N, 6.48.

***trans*-(BQA)RuH(PMe$_3$)$_2$ (14).** To a green solution of **11** (37 mg, 0.066 mmol) in toluene (5 mL) was added 68 μL of a 0.25 M solution of $LiAlH_4$ in THF at room temperature. The mixture was stirred at room temperature for 5 h, after which the volatiles were removed in vacuo. The residue was extracted into toluene and filtered through a Celite pad. The volatiles were removed in vacuo, and the solid obtained was triturated with petroleum ether to give an analytically pure, black-green solid (26 mg, 75%). Scaling this reaction resulted in drastically diminished yields. ^{1}H NMR (C_6D_6, 300 MHz): δ 8.44 (br, s, 2H), 7.87−7.84 (m, 2H), 7.39−7.28 (m, 4H), 6.75−6.72 (m, 2H), 6.37−6.33 (m, 2H), 0.80 (br, s, 18H), −11.75 (t, $^2J_{P-H}$ = 27.4 Hz). ^{31}P{^{1}H} NMR (C_6D_6, 121 MHz): δ 1.47. IR (Nujol mull/KBr): ν_{Ru-H} 1743.0 cm^{-1}. Anal. calcd for $C_{24}H_{31}N_3P_2Ru$: C, 54.95; H, 5.96; N, 8.01. Found: C, 54.99; H, 5.88; N, 7.96.

***trans*-(BQA)RuMe(PMe$_3$)$_2$ (15).** A green solution of **11** (0.10 g, 0.19 mmol) in toluene (5 mL) was treated with 3.5 equiv of MeLi (1.0 M) in diethyl ether at −30 °C. The mixture was then heated at 60 °C for 12 h. The reaction mixture was cooled to room temperature, and the excess MeLi was quenched with ethanol. The volatiles were then removed in vacuo. The resulting residue was extracted with benzene and filtered through a pad of Celite. The filtrate was concentrated in vacuo, triturated with petroleum ether, and dried in vacuo to yield a green solid (51 mg, 50%). ^{1}H NMR (C_6D_6, 300 MHz): δ 8.28−8.26 (m, 2H), 7.84−7.81 (m, 2H), 7.37−7.30 (m, 4H), 6.75−6.72 (m, 2H), 6.47−6.42 (m, 2H), 0.57 (t, J = 2.7 Hz, 18H, P(CH_3)$_3$), 0.01 (t, J = 9.8 Hz, 3H, RuCH_3). ^{31}P{^{1}H} NMR (C_6D_6, 121 MHz): δ 3.18. Anal. calcd $C_{25}H_{33}N_3P_2Ru$: C, 55.75; H, 6.18; N, 7.80. Found: C, 55.36; H, 6.00; N, 7.78.

***trans*-(BQA)RuN$_3$(PMe$_3$)$_2$ (16).** A green solution of **11** (0.10 g, 0.19 mmol) in 10 mL of CH_2Cl_2 was treated with solid sodium azide (48 mg, 0.70 mmol). The mixture was stirred at 50 °C for 4 h. The volatiles were then removed in vacuo. The resulting residue was extracted with benzene and filtered through a pad of Celite. The filtrate was concentrated in vacuo, triturated with petroleum ether, and dried in vacuo to yield a green solid (64 mg, 64%). ^{1}H NMR (C_6D_6, 300 MHz): δ 8.78−8.75 (m, 2H), 7.66−7.63 (m, 2H), 7.31−7.20 (m, 4H), 6.72−6.69 (m, 2H), 6.59−6.54 (m, 2H), 0.56 (t, J = 3.0 Hz, 18H). ^{31}P{^{1}H} NMR (C_6D_6, 121 MHz): δ 1.66. IR (Nujol/KBr): ν_{N3} = 2028.1 cm^{-1}. Anal. calcd for $C_{24}H_{30}N_6P_2Ru$: C, 50.97; H, 5.35; N, 14.86. Found: C, 51.14; H, 5.23; N, 14.40.

3,5-(CF$_3$)$_2$Ph-QAH (17). A 200 mL reaction vessel equipped with a Teflon stopcock and stir bar was charged with $Pd_2(dba)_3$ (0.218 g, 0.238 mmol), 1,1′-bis(diphenylphosphino)ferrocene (DPPF) (0.264 g, 0.476 mmol), and toluene (30 mL) under a dinitrogen atmosphere. The resulting solution was allowed to stir for 5 min, after which 3,5-bis(triflouromethyl)bromobenzene (3.49 g, 11.9 mmol), 8-aminoquinoline (2.48 g, 11.9 mmol), and additional toluene (70 mL) were added. The subsequent addition of sodium *tert*-butoxide (1.60 g, 16.66 mmol) resulted in a brown solution that was stirred vigorously for three days at 110 °C under a vacuum. The solution was then allowed to cool and filtered through a silica plug that was then extracted with dichloromethane to ensure complete removal of the desired product. Concentration of the collected extracts and removal of the solvent yielded a crude red solid (3.98 g, 94%). Purification by flash chromatography on silica gel (4:1 toluene/ethyl acetate) yielded a burgundy red liquid as a spectroscopically pure and synthetically useful compound (3.7 g, 87%). ^{1}H NMR (C_6D_6, 300 MHz, 25 °C): δ 8.50 (dd, J = 1.8, 4.2 Hz, 1H), 8.40 (s, *1*H), 7.53 (dd, J = 1.8, 8.4 Hz, 1H), 7.36 (m, J = 0.9 Hz, 1H), 7.28 (s, 2H), 7.23 (dd, J = 1.5, 7.2 Hz, 1H), 6.95−7.04 (m, 2H), 6.82 (dd, J = 4.2, 4.2 Hz, 1H). ^{13}C NMR (C_6D_6, 75.409 MHz, 25 °C): δ 148.1, 144.2, 139.6, 138.7, 136.5, 133.3, 132.9, 129.5, 127.6, 126.1, 122.4, 119.4, 118.2, 114.5 (m), 110.1. ^{19}F NMR (C_6D_6, 282.127 MHz, 25 °C): δ −63.4. ES-MS (electrospray): calcd for $C_{17}H_{10}F_6N_2$ $(M)^+$ *m/z* 356, found $(M + H)^+$ *m/z* 357.

[3,5-(CF$_3$)$_2$-(C$_6$H$_3$)QA][Na(Et$_2$O)] (18). A suspension of NaH (60% by weight; 57 mg, 1.4 mmol) in Et_2O (2 mL) was added to a solution of 3,5-$(CF_3)_2$Ph-QAH (500 mg, 1.4 mmol) in Et_2O (4 mL). Upon heating to reflux, a red-orange salt precipitated. After 10 h of heating, the reaction was cooled to room temperature, and the solvent decanted away. The salt was washed with petroleum ether (4 × 5 mL) and dried in a vacuum to afford an orange powder (544 mg, 86%). Hydrolysis of the salt with water cleanly affords the parent amine. ^{1}H NMR (C_6D_6, 300 MHz, 25 °C): δ 7.58 (dd, J = 1.8, 4.2 Hz, 1H), 7.49 (dd, J = 1.8, 8.4 Hz, 1H), 7.38 (dd, J = 1.2, 7.8 Hz, 1H), 7.18 (t, J = 7.8 Hz, 1H), 7.12 (s, 1H), 7.08 (s, 2H), 6.84 (dd, J = 1.2, 7.8 Hz, 1H), 6.65 (dd, J = 4.2, 8.4 Hz, 1H), 3.01 (q, $(CH_3CH_2)_2O$ J = 7.2 Hz, 4H), 0.86 (t, $(CH_3CH_2)_2O$ J = 7.2 Hz, 6H). ^{19}F NMR (C_6D_6, 282.127 MHz, 25 °C): δ −65.

(BQA)Ru(3,5-(CF$_3$)$_2$-(C$_6$H$_3$)QA)(PPh$_3$) (19). A solution of **18** (245.1 mg, 0.54 mmol) in THF (2 mL) was added dropwise to a stirring solution of **5** (500 mg, 0.54 mmol) in THF (4 mL). The reaction solution was heated to 80 °C for 3 h. The reaction was then cooled to room temperature and the volatiles removed in vacuo. The purple solid was washed with a 3:1 petroleum ether and ethanol mix (3 × 5 mL). The remaining solid was dried in vacuo, yielding 476 mg of analytically pure material (90%). Crystals were grown by cooling a solution of **19** in benzene layered with petroleum ether. ^{1}H NMR (C_6D_6, 300 MHz, 25 °C): δ 8.99 (dd, J = 1.2, 4.8 Hz, 1H), 7.57 (dd, J = 1.2, 4.8 Hz, 2H), 7.49 (dd, J = 1.2, 8.2 Hz, 1H), 7.19 (d, J = 1.2 Hz, 1H), 6.77−7.08 (m, 14H), 6.75 (m, 6H), 6.58−6.64 (m, 5H), 6.53 (dd, J = 5.4, 7.2 Hz, 1H), 6.44 (s, 2H),

6.08 (dd, $J = 4.8$, 8.2 Hz, 2H). ^{31}P {^{1}H} NMR (C_6D_6, 121.4 MHz, 25 °C): δ 50.5. ^{19}F NMR (C_6D_6, 282.127 MHz, 25 °C): δ −64. ES-MS (electrospray): calcd for $C_{53}H_{36}F_6N_5PRu$ $(M)^+$ m/z 988, found $(M + H)^+$ m/z 989. Anal. calcd for $C_{53}H_{36}F_6N_5PRu$: C, 64.37; H, 3.67; N, 7.08. Found: C, 64.38; H, 3.64; N, 7.08.

(BQA)Ru(3,5-(CF$_3$)$_2$-(C$_6$H$_3$)QA)(CO) (20). A 100 mL reaction vessel equipped with a Teflon stopcock and stir bar was charged with a solution of **19** (50 mg, 0.05 mmol) in toluene (15 mL). The reaction vessel was evacuated and then exposed to 1 atm of CO gas. The reaction mixture was heated at reflux with vigorous stirring for 8 h. The reaction was then cooled to room temperature and the volatiles removed in vacuo. The red solid was washed with a 3:1 petroleum ether and ethanol mix (3 × 5 mL). The remaining solid was dried in vacuo, yielding 36 mg of analytically pure material (95%). ^{1}H NMR (C_6D_6, 300 MHz, 25 °C): δ 9.01 (dd, $J = 1.2$, 4.8 Hz, 1H), 7.50 (dd, $J = 1.2$, 4.8 Hz, 2H), 7.48 (dd, $J = 1.2$, 8.2 Hz, 1H), 7.20 (d, $J = 1.2$ Hz, 1H), 6.58−7.08 (m, 11H), 6.52 (dd, $J = 5.4$, 7.2 Hz, 1H), 6.44 (s, 2H), 6.08 (dd, $J = 4.8$, 8.2 Hz, 2H). ^{19}F NMR (C_6D_6, 282.127 MHz, 25 °C): δ −64. Anal. calcd for $C_{36}H_{21}F_6N_5ORu$: C, 57.30; H, 2.80; N, 9.28. Found: C, 57.02; H, 2.78; N, 9.18.

[(BQA)RuCl(PhBP$_2$)][NEt$_4$] (21). A solution of $[Ph_2B(CH_2PPh_2)_2][NEt_4]$ (354 mg, 0.51 mmol) in THF (2 mL) was added dropwise to a stirring solution of **5** (471 mg, 0.51 mmol) in THF (4 mL). The reaction solution was heated to 80 °C for 3 h. The reaction was then cooled to room temperature and the solvent removed in vacuo. The dark purple solid was washed with Et_2O (2 × 15 mL) and petroleum ether (2 × 15 mL). The remaining solid was dried in vacuo, yielding 497 mg of analytically pure material (89%). Crystals of **21** were grown by vapor diffusion of petroleum ether into THF. ^{1}H NMR (C_6D_6, 300 MHz, 25 °C): δ 8.46 (bs, 4H), 7.93 (bs, 2H), 7.75 (bs, 2H), 7.49 (d, $J = 6.3$ Hz, 2H), 6.95−7.39 (m, 18H), 6.79 (t, $J = 7.2$ Hz, 5H), 6.67 (t, $J = 7.2$ Hz, 4H), 6.36−6.47 (m, 9H), 3.29 (q, $J = 7.5$ Hz, 8H), 2.35 (bs, 2H), 1.81 (bs, 2H), 1.23 (tt, $J = 1.5$, 7.2 Hz, 12 H). ^{31}P {^{1}H} NMR (C_6D_6, 121.4 MHz, 25 °C): δ 54 (d, $J = 36$ Hz), 28.3 (d, $J = 36$ Hz). ^{11}B {^{1}H} NMR (C_6D_6, 128.3 MHz, 25 °C): δ −11.8. Anal. calcd for $C_{64}H_{66}BClN_4P_2Ru$: C, 69.85; H, 6.04; N, 5.09. Found: C, 69.78; H, 6.05; N, 5.08.

(BQA)Ru[Ph$_2$BP$_2$] (22). Solid **21** (100.6 mg, 0.09 mmol) was stirred vigorously in ethanol (6 mL) for 30 min. A red solid precipitated from solution and was isolated by decanting the liquor away. The solids were dissolved in CH_2Cl_2 and filtered through a pad of Celite. The solvent was removed in vacuo, and the remaining wine red solid was washed with petroleum ether (2 × 3 mL) and dried in vacuo, yielding 72 mg of analytically pure material (84%). ^{1}H NMR (C_6D_6, 300 MHz, 25 °C): δ 8.17 (s, 5 H), 7.72 (d, $J = 4.8$ Hz, 2H), 7.54 (m, 10 H), 7.30 (d, $J = 6$ Hz, 4H), 7.04 (d, $J = 8.7$ Hz, 2H), 6.851 (d, $J = 7.8$ Hz, 2H), 6.50 (m, 10 H), 6.2 (m, 2 H), 5.81 (m, 2 H), 2.69 (s, 4 H). ^{31}P {^{1}H} NMR (C_6D_6, 121.4 MHz, 25 °C): δ 69.45. ^{11}B {^{1}H} NMR (C_6D_6, 128.3 MHz, 25 °C): δ −12.1. Anal. calcd for $C_{56}H_{46}BN_3P_2Ru$: C, 71.95; H, 4.96; N, 4.50. Found: C, 71.78; H, 5.05; N, 4.44.

(BQA)Ru(CO)(PhBP$_2$) (23). A 20 mL vial containing **21** (60 mg, 0.054 mmol) in CH_2Cl_2 (2 mL) was sparged with CO gas. The solution instantly reddened upon contact with the gas. The solvent was removed in vacuo, and the remaining red solid was washed with ethanol (2 × 2 mL). The resulting powder was washed with petroleum ether (2 × 3 mL) and dried in vacuo, yielding 45 mg of analytically pure material (86%). ^{1}H NMR (C_6D_6, 300 MHz, 25 °C): δ 7.90 (m, 4 H), 7.75 (d, $J = 4.5$ Hz, 2H), 7.53 (d, $J = 7.2$ Hz, 2 H), 7.32 (d, $J = 8.1$ Hz, 2H), 7.11−7.22 (m, 8H), 7.04 (t, $J = 7.5$ Hz, 4H), 6.92 (s, 6 H), 6.67 (t, $J = 6.6$ Hz, 2 H), 6.53 (d, $J = 7.5$ Hz, 2 H), 6.27−6.44 (m, 10 H), 2.78 (d, $J = 12$ Hz, 2 H), 2.02 (d, $J = 13.8$ Hz, 2 H). ^{13}C NMR (C_6D_6, 75.409 MHz, 25 °C): δ 155, 151, 149, 137, 135, 133.2, 133.1, 132.6, 132.5, 131, 129, 128.5, 128.4, 128, 127, 126.8, 126.7, 123, 120, 114. ^{31}P {^{1}H} NMR (C_6D_6, 121.4 MHz, 25 °C): δ 35.17 (d, $J = 35$ Hz), 18.81 (d, $J = 35$ Hz). ^{11}B {^{1}H} NMR (C_6D_6, 128.3 MHz, 25 °C): δ −11.9. IR: (CH_2Cl_2) $\nu_{CO} = 1970$ cm^{-1}. Anal. calcd for $C_{57}H_{46}BN_3OP_2Ru$: C, 71.10; H, 4.82; N, 4.36. Found: C, 71.06; H, 4.70; N, 4.28.

[*trans*-(BQA)Ru(CO)(PPh$_3$)$_2$][BPh$_4$] (25). $NaBPh_4$ (18.2 mg, 0.05 mmol) in ethanol (1 mL) was added to a solution of **5** (45 mg, 0.05 mmol) in THF (2 mL) in a 10 mL Schlenk flask equipped with a stir bar and septum. The flask was evacuated, then exposed to 1 atm of CO gas. The green solution reddens instantly upon exposure to CO. The reaction was allowed to stir for 30 min before the volatiles were removed in vacuo. The red solid was washed with ethanol (2 × 3 mL) and Et_2O (2 × 3 mL). The remaining solid was dried in vacuo, yielding 49 mg of analytically pure material (82%). ^{1}H NMR (C_6D_6, 300 MHz, 25 °C): complex pattern of resonances between 8.55 and 6.98 ppm (62H). ^{31}P {^{1}H} NMR (C_6D_6, 121.4 MHz, 25 °C): δ 30.1. IR: (CH_2Cl_2/KBr): ν_{CO} 1970 cm^{-1}. ES-MS (electrospray): calcd for $C_{55}H_{42}N_3OP_2Ru$ $(M)^+$ m/z 924, found $(M)^+$ m/z 924, 662 (M − PPh_3). Anal. calcd for $C_{79}H_{62}BN_3OP_2Ru$: C, 76.32; H, 5.03; N, 3.38. Found: C, 76.15; H, 4.87; N, 3.36.

[*trans*-(BQA)Ru(CH$_3$CN)(PPh$_3$)$_2$][BPh$_4$] (24). A solution of **5** (88 mg, 0.094 mmol) in a mixture of acetonitrile and methanol (2 mL/4 mL) was added to a solution of $NaBPh_4$ (51 mg, 0.15 mmol) in methanol (2 mL) at room temperature. The resulting mixture was stirred at room temperature for 4 h; then, the volatiles were removed in vacuo. The solid residue was extracted with dichloromethane (5 mL) and filtered through a Celite pad. The volatiles were removed in vacuo, and the purple solid was triturated with petroleum ether. The solids were dried in vacuo to afford 78 mg of analytically pure material (67%). ^{1}H NMR ($CDCl_3$, 300 MHz, 25 °C): complex pattern of resonances between 8.48 and 7.00 ppm (62H). ^{31}P{^{1}H} NMR ($CDCl_3$, 121 MHz) δ 28.7 (bs). Anal. calcd for $C_{78}H_{62}BN_3P_2Ru$: C, 77.09; H, 5.14; N, 3.46. Found: C, 77.48; H, 5.69; N, 3.69.

[*trans*-(BQA)Os(CO)(PPh$_3$)$_2$][PF$_6$] (26). A solution of $TlPF_6$ (13.6 mg, 0.02 mmol) in THF (1 mL) was added to a solution of **6** (40 mg, 0.02 mmol) in THF (2 mL) in a 10 mL Schlenk flask equipped with a stir bar and septum. The flask was evacuated, then exposed to 1 atm of CO gas. The green solution reddens after stirring vigorously over the period of 1 h. The reaction was allowed to stir for 5 h, and then the volatiles were removed in vacuo. The red solid was washed with ethanol (2 × 3 mL) and Et_2O (2 × 3 mL). The remaining solid was dried in vacuo, yielding 48 mg of analytically pure material (90%). ^{1}H NMR (C_6D_6, 300 MHz, 25 °C): complex pattern of resonances between 8.58 and 6.56 ppm (42H). ^{31}P {^{1}H} NMR (C_6D_6, 121.4 MHz, 25 °C): δ 0.31. IR: (CH_2Cl_2/KBr) $\nu_{CO} = 1921$ cm^{-1}. ES-MS (Electrospray): calcd for $C_{55}H_{42}N_3OOsP_2$ $(M)^+$ m/z 1013, found $(M)^+$ m/z 1014. Anal. calcd for $C_{55}H_{42}F_6N_3OOsP_3$: C, 57.04; H, 3.66; N, 3.63. Found: C, 56.64; H, 3.51; N, 3.60.

[*trans*-(BQA)RuCl(PPh$_3$)$_2$][OTf] (27). To a vigorously stirring solution of **5** (0.11 g, 0.12 mmol) in toluene (5 mL) was added solid AgOTf (30 mg, 0.12 mmol) at room temperature. The reaction mixture turned brown instantly, while a black precipitate formed. After the mixture was stirred for 1 h, the solution was filtered through a Celite pad to remove the precipitate. The volatiles were removed in vacuo. The solids were then extracted into CH_2Cl_2 (5 mL) and filtered again through a Celite pad. The volume of the filtrate was reduced to 1 mL, layered with diethyl ether, and allowed

to stand. A yellow precipitate formed and was isolated by decanting the liquor. The solids were dried in vacuo to afford analytically pure material (0.12 g, 93%). ES-MS (electrospray): calcd for $C_{54}H_{42}ClN_3P_2Ru$ $(M)^+$ *m/z* 931, found $(M + H)^+$ *m/z* 931. Anal. calcd for $C_{55}H_{42}ClF_3N_3O_3P_2RuS$: C, 61.14; H, 3.92; N, 3.89. Found: C, 60.81; H, 3.70; N, 3.76.

[*trans*-(BQA)Ru(N$_2$)(PPh$_3$)$_2$][PF$_6$] (30). $TlPF_6$ (18.8 mg, 0.054 mmol) in THF (1 mL) was added to a solution of **5** (50 mg, 0.054 mmol) in THF (2 mL) at room temperature. The green solution darkens to a midnight blue after stirring for several hours, and the evolution of a white precipitate is noticeable. The reaction mixture was allowed to stir for 24 h and was filtered through a Celite pad, and then the volatiles were removed in vacuo. Dissolution of the blue solids in CH_2Cl_2 caused a color change to an intense red. The solution was filtered through a Celite pad, and the volatiles were removed in vacuo. The red solid was washed with Et_2O (2 × 3 mL). The remaining solid was dried in vacuo, yielding 56 mg of analytically pure material (83%). ^{1}H NMR (CD_2Cl_2, 300 MHz, 25 °C): complex pattern of resonances between δ 8.64 and 7.04 (42H). ^{31}P {^{1}H} NMR (CD_2Cl_2, 121.4 MHz, 25 °C): δ 25, −143 (sept, J = 711 Hz). ES-MS (electrospray): calcd for $C_{54}H_{42}ClN_5P_2Ru$ $(M)^+$ *m/z* 924, found $(M + H)^+$ *m/z* 896 $(M - N_2)^+$. IR: (CH_2Cl_2/KBr): ν_{NN} 2130 cm^{-1}. Anal. calcd for $C_{54}H_{42}F_6N_5P_3Ru$: C, 60.68; H, 3.96; N, 6.55. Found: C, 60.55; H, 3.90; N, 6.48.

[*trans*-(BQA)Ru(N$_2$)(PMe$_3$)$_2$][PF$_6$] (31). $TlPF_6$ (18.8 mg, 0.054 mmol) in THF (1 mL) was added to a solution of **5** (30 mg, 0.054 mmol) in THF (2 mL) at room temperature. The green solution reddens after stirring for several hours, and the evolution of a white precipitate is noticeable. The reaction mixture was allowed to stir for 36 h and was filtered through a Celite pad, and then the volatiles were removed in vacuo. The solids were dissolved in CH_2Cl_2 and filtered through a Celite pad, and the volatiles were removed in vacuo. The red solid was washed with Et_2O (2 × 3 mL). The remaining solid was dried in vacuo, yielding 36 mg of analytically pure material (78%). ^{1}H NMR (CD_2Cl_2, 300 MHz, 25 °C): δ 8.35 (d, J = 5.1 Hz, 2H), 8.04 (d, J = 7.8 Hz, 2H), 7.91 (d, J = 7.8 Hz, 2H), 7.54 (t, J = 7.8 Hz, 2H), 7.25 (dd, J = 7.8, 7.8 Hz, 2H), 7.04 (d, J = 7.8 Hz, 2H), 0.72 (t, J = 2.7 Hz, 18H). ^{31}P {^{1}H} NMR (CD_2Cl_2, 121.4 MHz, 25 °C): δ 0.42, −143 (sept, J = 711 Hz). ES-MS (electrospray): calcd for $C_{24}H_{30}N_5P_2Ru$ $(M)^+$ *m/z* 552, found $(M + H)^+$ *m/z* 524 $(M - N_2)^+$. IR (CH_2Cl_2/KBr): ν_{NN} 2129 cm^{-1}. Anal. calcd for $C_{24}H_{30}F_6N_5P_3Ru$: C, 41.39; H, 4.34; N, 10.05. Found: C, 41.29; H, 4.15; N, 9.89.

[*trans*-(BQA)Os(N$_2$)(PPh$_3$)$_2$][PF$_6$] (32). A solution of $TlPF_6$ (13.6 mg, 0.02 mmol) in THF (1 mL) was added to a solution of **6** (40 mg, 0.02 mmol) in THF (2 mL) at room temperature. The green solution reddens after stirring vigorously over a period of several hours. The reaction was allowed to stir for 24 h and was filtered through a Celite pad, and then the volatiles were removed in vacuo. The red solid was extracted into CH_2Cl_2 and filtered through a Celite pad. The volatiles were removed in vacuo, and the resultant solids were washed with Et_2O (2 × 3 mL). The remaining solid was dried in vacuo, yielding 48 mg of analytically pure material (89%). ^{1}H NMR (C_6D_6, 300 MHz, 25 °C): complex pattern of resonances between 8.47 and 6.44 ppm (42H). ^{31}P {^{1}H} NMR (C_6D_6, 121.4 MHz, 25 °C): δ −3.7. IR (CH_2Cl_2/KBr): ν_{NN} 2073 cm^{-1}. ES-MS (electrospray): calcd for $C_{54}H_{42}N_5OsP_2$ $(M)^+$ *m/z* 1013, found $(M)^+$ *m/z* 1014, 986 $(M - N_2)^+$. Anal. calcd for $C_{54}H_{42}F_6N_5OsP_3$: C, 56.00; H, 3.66; N, 6.05. Found: C, 55.92; H, 3.61; N, 5.99.

Acknowledgment. J.C.P. is grateful to the NSF for financial support of this work (CHE-0750234 and CHE-0132216). T.A.B. is grateful to the Department of Defense for a graduate research fellowship.

Supporting Information Available: Crystallographic data (PDF and CIF). This material is available free of charge via the Internet at http://pubs.acs.org.

IC801047S